



**HAL**  
open science

# Humidity Sensing with Supramolecular Nanostructures

Verónica Montes Garcia, Paolo Samorì

► **To cite this version:**

Verónica Montes Garcia, Paolo Samorì. Humidity Sensing with Supramolecular Nanostructures. *Advanced Materials*, 2023, pp.2208766. 10.1002/adma.202208766 . hal-04020470

**HAL Id: hal-04020470**

**<https://hal.science/hal-04020470v1>**

Submitted on 8 Mar 2023

**HAL** is a multi-disciplinary open access archive for the deposit and dissemination of scientific research documents, whether they are published or not. The documents may come from teaching and research institutions in France or abroad, or from public or private research centers.

L'archive ouverte pluridisciplinaire **HAL**, est destinée au dépôt et à la diffusion de documents scientifiques de niveau recherche, publiés ou non, émanant des établissements d'enseignement et de recherche français ou étrangers, des laboratoires publics ou privés.

# Humidity Sensing with Supramolecular Nanostructures

Verónica Montes-García and Paolo Samorì\*

Precise monitoring of the humidity level is important for the living comfort and for many applications in various industrial sectors. Humidity sensors have thus become one among the most extensively studied and used chemical sensors by targeting a maximal device performance through the optimization of the components and working mechanism. Among different moisture-sensitive systems, supramolecular nanostructures are ideal active materials for the next generation of highly efficient humidity sensors. Their noncovalent nature guarantees fast response, high reversibility, and fast recovery time in the sensing event. Herein, the most enlightening recent strategies on the use of supramolecular nanostructures for humidity sensing are showcased. The key performance indicators in humidity sensing, including operation range, sensitivity, selectivity, response, and recovery speed are discussed as milestones for true practical applications. Some of the most remarkable examples of supramolecular-based humidity sensors are presented, by describing the finest sensing materials, the operating principles, and sensing mechanisms, the latter being based on the structural or charge-transport changes triggered by the interaction of the supramolecular nanostructures with the ambient humidity. Finally, the future directions, challenges, and opportunities for the development of humidity sensors with performance beyond the state of the art are discussed.

## 1. Introduction

The precise control of moisture in air is fundamental for many applications including air conditioning systems, mining sector,<sup>[1]</sup> agriculture<sup>[2]</sup> or (bio)medical<sup>[3]</sup> technologies as well as for chemical,<sup>[4]</sup> pharmaceutical,<sup>[5]</sup> automotive, cement, and food industry.<sup>[6]</sup> Rooted by the ever-increasing search for optimization of these applications, along with the huge drive toward improving the quality of our lives, the market for humidity sensors continues to grow and the fields of application are simultaneously fast expanding.<sup>[7]</sup> The gigantic demand for devices

capable of monitoring and controlling the humidity level has triggered the development of smaller, more reliable, and better-performing humidity sensors.<sup>[8]</sup>


The advancement in the performance of humidity sensors encompasses an improvement of the transducer characteristics including sensing elements, structure design, the principle of mechanism, and fabrication technologies.<sup>[1]</sup> In this context, advanced sensing elements are key to achieving state-of-the-art performance. Hitherto, different active materials have been explored, including ceramics,<sup>[9]</sup> carbon-based materials,<sup>[10]</sup> composites and organic/polymeric thin films.<sup>[1,11]</sup> Despite the many attractive potential uses of these materials as humidity sensors, they exhibit some unavoidable drawbacks which have stymied their use in practical applications. For instance, ceramic materials frequently possess certain level of toxicity, poor biocompatibility, long response and recovery times, low sensitivity and high hysteresis. Carbon-based materials exhibit low selectivity, poor reproducibility, and possible long-term drift. Most of the concerns on

organic/polymeric materials are related to water solubility at high humidity level, low degree of sensitivity at low humidity, and hysteresis modifications.

Supramolecular nanostructures have emerged during the last decade as ideal components for the next generation of highly efficient humidity sensors. Built via the noncovalent interactions among rationally designed artificial or natural molecular units, supramolecular nanostructures can be integrated into organic functional systems or can be combined with inorganic materials yielding hybrid systems via functionalization with appropriate chemical groups. Inspired by nature, scientists have tried over the last two decades to understand and emulate biological systems for generating more and more complex supramolecular architectures capable of recognizing target molecules with high affinity and specificity.<sup>[12]</sup> Therefore, through the proper design in terms of size, geometry, dipole and quadrupole moments, and surface charges, supramolecular nanostructures can act as ad hoc chemical receptors of the chosen analyte. Humidity sensing occurs via recognition events between suitably designed supramolecular receptors and water molecules, and it is accompanied by a variation in the optical properties, mass, or electrical characteristics of the system. Importantly, reversible noncovalent interactions guarantee quick responses and fast recovery rates, which are required to enable continuous humidity monitoring. Although

V. Montes-García, P. Samorì  
Université de Strasbourg  
CNRS

ISIS UMR 7006, 8 allée Gaspard Monge, Strasbourg F-67000, France  
E-mail: samori@unistra.fr

 The ORCID identification number(s) for the author(s) of this article can be found under <https://doi.org/10.1002/adma.202208766>.

© 2023 The Authors. Advanced Materials published by Wiley-VCH GmbH. This is an open access article under the terms of the Creative Commons Attribution License, which permits use, distribution and reproduction in any medium, provided the original work is properly cited.

DOI: 10.1002/adma.202208766

supramolecular chemistry has been used for the detection of volatile compounds for almost thirty years, its use for humidity sensing has only emerged during the last ten years.

In view of the rapid growth of this field of materials science, here we provide a perspective of the state of the art of humidity sensors with supramolecular nanostructures. We first discuss the different key performance indicators in humidity sensing, correlating them to specific application fields. Then, we highlight representative examples of these supramolecular nanostructures by discussing the different sensing mechanisms that have been explored in order to improve the sensing performances. We examine the major benefits, progress, and limitations derived from the rational design of supramolecular nanostructures for high-performing humidity sensing and practical applications. We identify future directions, challenges, and opportunities to expand the frontiers of supramolecular nanostructures-based humidity sensors toward technologies with potential impact on environmental sciences and biomedical applications.

## 2. Characteristics and Key Performance Indicators

Humidity is defined as the amount of water vapor in an atmosphere of air or other gases. Humidity parameters are expressed in different ways and the corresponding units are based on the measurement technique used. The most commonly used

parameter is relative humidity (RH), defined as the ratio of the amount of moisture content of air to the maximum (saturated) moisture level that the air can hold at the same given temperature and pressure of the gas.

The first parameter to be considered when fabricating a humidity sensor is the desired operation range, which depends entirely on the application (Figure 1a). Under standard living conditions, the RH is normally kept around 40–60% to be considered comfortable. However, specific applications may require a different RH level. For instance, the RH must be constantly set between  $\approx 35$ –40% in clean rooms,  $\approx 12\%$  in planes, and  $\approx 60\%$  in hospital surgery rooms. In environments where the humidity is higher than 50%, electronics are susceptible to damage. Moreover, the RH must be kept close to 0% for operating with certain equipment, such as high-impedance electronic circuits, high-voltage devices, or electrostatic-sensitive components. While in some applications a broad operation range may be desirable (e.g., climatology), other applications require a very specific operation range (e.g., industrial or biomedical applications).

Once the operation range is defined, the next parameter to be considered is the sensor sensitivity (Figure 1b). In humidity sensors, the sensitivity indicates the capability of the sensor to differentiate between two very close RH levels. This parameter, which can be critical for some applications, is sometimes overlooked. However, quantifying the humidity sensor sensitivity, i.e., the fitting curve slope, is challenging, as some sensors

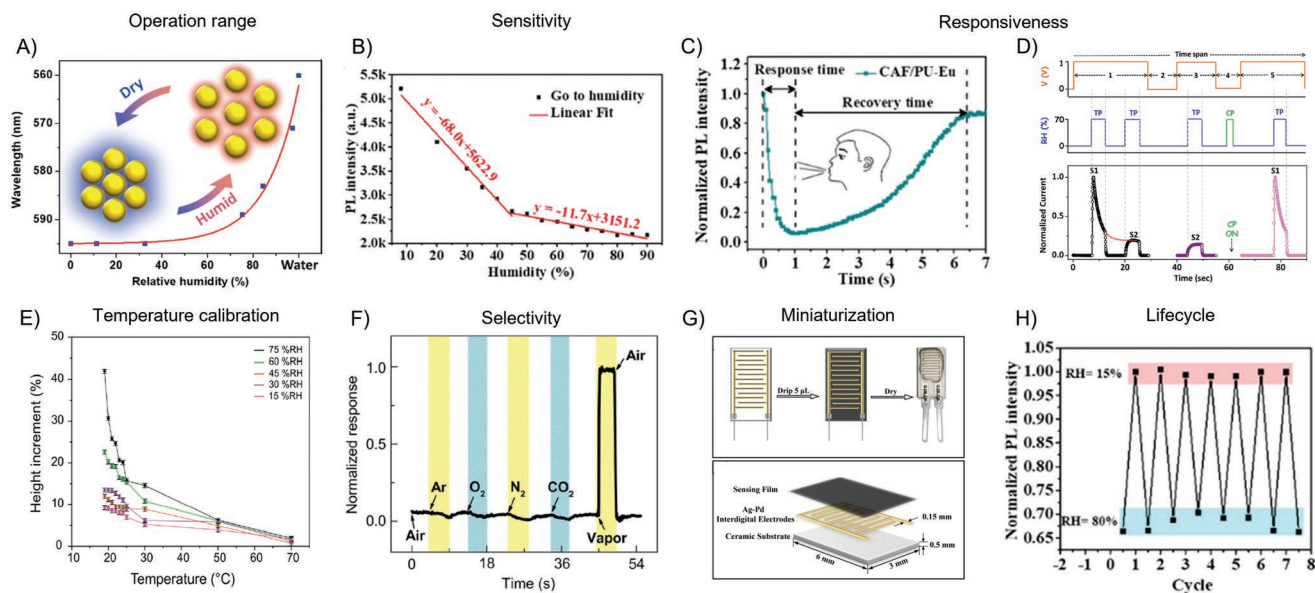


**Figure 1.** Key performance indicators of humidity sensors. A) Operation range. Response (i.e., absorbance) of a colorimetric humidity sensor as a function of the operation range, from 0% RH to water level. Reproduced with permission.<sup>[18]</sup> Copyright 2019, Royal Society of Chemistry. B) Sensitivity. Response (i.e., photoluminescence) of a humidity sensor as a function of the humidity level. The response was linearly fitted in two different humidity regimes. Reproduced with permission.<sup>[19]</sup> Copyright 2020, American Chemical Society. C, D) Responsiveness. C) Response and recovery time of a humidity sensor for real-time monitoring. Reproduced with permission.<sup>[19]</sup> Copyright 2020, American Chemical Society. D) Response and recovery time of a moisture memory humidity sensor. Reproduced with permission.<sup>[20]</sup> Copyright 2017, American Chemical Society. E) Temperature calibration. Response (i.e., height level) of a humidity sensor as a function of the humidity level at different temperatures. Reproduced with permission.<sup>[21]</sup> Copyright 2020, American Chemical Society. F) Selectivity. Response of a humidity sensor to different gases. Reproduced with permission.<sup>[22]</sup> Copyright 2020, Wiley-VCH. G) Miniaturization. Chemiresistor humidity sensor fabrication with low dimensions. Reproduced under the terms of the CC-BY Creative Commons Attribution 4.0 International license (<https://creativecommons.org/licenses/by/4.0>).<sup>[23]</sup> Copyright 2017, The Authors, published by Springer Nature. H) Lifecycle. Response (i.e., photoluminescence) of a humidity sensor after several humidity cycles. Reproduced with permission.<sup>[19]</sup> Copyright 2020, American Chemical Society.

do not exhibit a humidity response with a well-defined trend (e.g., linear, logarithmic, exponential). In those cases, the ratio between the signal at the highest and the lowest humidity level is frequently reported.<sup>[13]</sup>

The response and recovery time of the output signal and the reversibility are also of paramount importance (Figure 1c,d). A sensor exhibiting good reversibility together with a fast response and recovery time (typically a fraction of a second) can be employed in situations where the RH level may change dynamically (Figure 1c).<sup>[14]</sup> Such application areas include industrial process controls, meteorology and various medical diagnostics including monitoring human exhaled breath. In particular, real-time monitoring of respiratory rate (RR) is highly important for human health, clinical diagnosis, and fundamental scientific research.<sup>[14–15]</sup> In recent years, the development of a second type of humidity sensors, displaying moisture memory, has emerged.<sup>[16]</sup> The exposure of these sensors to a certain RH level would trigger a fast response (i.e., change in optical or electrical properties), that is kept in time. Only when an external stimulus (e.g., temperature) is applied, the system will recover its initial state (Figure 1d).<sup>[17]</sup> These sensors are particularly important from the point of view of transporting and storing humidity-sensitive goods. In the case of a critical overexposure to humidity, this sensor would allow the verification in any stage of transport or storage prior to receiving the good.<sup>[16]</sup>

An important requirement for commercial competitiveness is the sequential enhancement of quality and devices' reliability (Figure 1e,f). For humidity sensors, it is essential to monitor, detect and control the ambient humidity under different conditions ranging from low temperature to high (Figure 1e) or in mixtures with other gases depending on the application (Figure 1f). Nowadays, simulation techniques are frequently used to predict and improve the output data before the implementation of mass production processes. However, to guarantee the proper degree of reliability of each sensor, calibration prior to real applications is required.

Device miniaturization offers numerous advantages, for instance, batch production, straightforward integration in other equipment (e.g., humidifiers), lower hysteresis, and lower production cost (Figure 1g).<sup>[16]</sup> In recent years, the use of nanomaterials together with the improvements in sensor manufacturing technologies (e.g., low-power and low-cost microelectronic hybrid circuits or modern signal conditioning methods) had led to major advances in miniaturization technologies.<sup>[16]</sup> Other characteristics of humidity sensors are common to all chemical sensors, including lifecycle (Figure 1h), low production costs, low environmental impact, etc.<sup>[12]</sup> Nevertheless, the engineering of novel device architectures is beyond the scope herein.

### 3. Operating Principle

The typical design of an electrical humidity sensor consists of a solid substrate, interdigitated electrodes, and the sensing material placed in-between the interdigitated electrodes. Different parameters such as resistance, capacitance, impedance, voltage, etc., can be recorded as a function of the RH level.<sup>[23–24]</sup> The properties of electrical humidity sensors are determined by the

hygroscopic sensing material used and by the device architecture (including geometry of the electrodes).

Piezoresistive humidity sensors are a subcategory of electrical humidity sensors. The piezoresistive principle is based on the change in the electrical resistivity of a material under mechanical stress. In this case, the presence of the RH causes the expansion or contraction of the material, leading to a stress change which then is transduced into an electrical readout. Although electrical readout has been widely used in supramolecular nanostructures, to the best of our knowledge, the piezoresistive principle has not been used as readout for any supramolecular nanostructure.

Electrical humidity sensors are currently the market-dominating technology. However, the use of a simple and clear optical readout with no need of power supply represents a very promising alternative. Different from conventional electrical humidity-responsive materials, in optical humidity sensors a clear color change can be observed by the naked eye of any untrained observer, since it does not require any extra instrumentation or interpretation.<sup>[25]</sup> Nevertheless, the accessibility to smart phones and digital cameras capable to record images and movies with a high resolution are instrumental to record and quantify color changes. Hence even assisting color blind users in identifying chromatic changes as a result of humidity variations. A measurable intrinsic color change could be beneficial in microelectromechanical systems or microrobots enabling a facile real-time verification of their status.

### 4. Materials

With the advancement of nanoscience and nanotechnology, a plethora of low-dimensional, supramolecularly engineered materials has been used as efficient humidity sensors by taking advantage of their high surface-to-volume ratio and surface sensitive properties which make them very susceptible to changes in the environments, hence rendering them particularly suitable for chemical sensing. This includes 0D systems (such as gold nanoparticles (AuNPs)),<sup>[24a]</sup> 1D systems (small molecules, and polymers),<sup>[26]</sup> and 2D systems (metal–organic frameworks/covalent organic frameworks, graphene, and related materials)<sup>[27]</sup> which can be functionalized with ad hoc receptors thereby becoming ideal sensory components to be readily integrated into devices.

Supramolecular chemistry offers a broadest arsenal of highly selective receptors of any analyte of interest. For the specific case of H<sub>2</sub>O molecules, functional humidity-sensitive moieties, including hydroxyl,<sup>[28]</sup> carboxyl,<sup>[29]</sup> and nitro groups,<sup>[28]</sup> quaternary ammonium,<sup>[30]</sup> sulfonate,<sup>[23]</sup> or phosphonium salts,<sup>[31]</sup> and vinyl alcohol<sup>[32]</sup> and ethylene glycol units<sup>[18]</sup> have shown to be ideal scaffolds, exhibiting hygroscopicity and undergoing reversible structural changes upon specific interaction with moisture.

### 5. Supramolecular Humidity Sensors

The moisture–materials interactions can be described by mainly three mechanisms (Figure 2). On the one hand, the

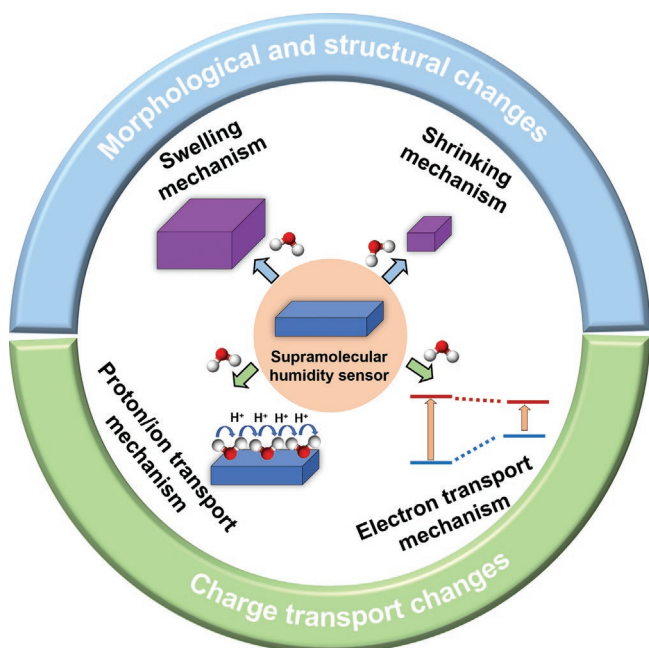


**Figure 2.** Illustration of the humidity sensing mechanisms by supramolecular nanostructures.

water uptake by the supramolecular nanostructures can trigger a modification of their morphology or structure (either swelling or shrinking) depending on the chemical/physical processes. On the other hand, when there are no major volume changes, humidity changes can induce modifications in the charge transport (protonic or electronic). In some cases, more than one mechanism can coexist, for instance, when a joint change in the volume of the system and proton/ionic conduction takes place, with this third mechanism being classified as hybrid mechanism.

## 5.1. Morphological and Structural Changes

### 5.1.1. Swelling Mechanism

The swelling mechanism is based on the adsorption and desorption of water into the supramolecular nanoporous structures, triggering an expansion of the material when the relative humidity increases. These changes can be monitored by both optical and electrical readout.

Herzer et al.<sup>[25]</sup> reported the fabrication of a printable H-bonded cholesteric liquid crystal (CLC) polymer film based on a mixture of both chemically (polymerizable acrylate groups) and physically (carboxylic acid groups, which form H-bonded dimers) crosslinkable groups (Figure 3a). The reactive mesogens C6M and LC756 acted as chemical crosslinker and chiral dopant, respectively, while 6OBA and 6OBA-M were the H-bonding molecular triggers (see Table 1 for complete chemical names). C6BP was added to decrease the crystalline-nematic phase transition. After a photopolymerization process, a hygroscopic CLC polymer salt was formed upon addition of a base (i.e., KOH 0.05 M for 10 min). This treatment triggered the

release of water from the CLC film, yielding a green-reflecting film. The exposure of these films to humidity resulted in reversible reflection color changes between green and yellow depending on the relative humidity (i.e., from 3% to 83% RH). The change in the reflection band was a result of a change in helix pitch in the film due to adsorption and desorption of water molecules, thereby inducing the swelling/shrinkage of the film material. Moreover, the authors printed the films on a foil, showing the potential application of supramolecular CLC materials as low-cost, printable, battery-free optical sensors.<sup>[25]</sup>

Following a similar strategy, del Pozo et al.<sup>[21]</sup> reported the fabrication of a photonic photoresist, based on a supramolecular CLC, for the generation of stimuli-responsive photonic moisture responsive microactuators via two-photon polymerization direct laser writing (Figure 3b). Micron-sized structures with different shapes, such as pillars, flowers or butterflies were fabricated. The controlled expansion of the microactuators at different temperatures and RH levels (i.e., between 42% and 75% RH) resulted in a corresponding shape and color change, owing to modulation of the nanoscale CLC pitch in the ordered network.<sup>[21]</sup>

Metallo-supramolecular polymers (MSPs), obtained by the 1:1 complexation of metal ions and ditopic organic ligands, have been devised as potential stimuli-responsive materials. Li et al.<sup>[19]</sup> reported the fabrication of an Eu-containing MSPs elastomer as a fast and ultrasensitive fluorescent-based humidity sensor. The rational design of this elastomer was based on the use of hygroscopic poly(tetramethylene ether glycol) (PTMG)-based polyurethane (PU) and europium ions ( $\text{Eu}^{3+}$ ) (PU-Eu). The urethane groups can coordinate  $\text{Eu}^{3+}$  inducing ligand-to-metal energy transfer and therefore emitting strong photoluminescence (PL). When this system was exposed to high RH, spontaneous hydration occurred as water molecules were quickly adsorbed by the hygroscopic PTMG segments of the PU-Eu elastomer. Once adsorbed, water molecules can compete with urethane groups to coordinate with  $\text{Eu}^{3+}$  ions, resulting in a decrease in the PL intensity. The PU-Eu elastomer with a thickness of 400  $\mu\text{m}$  displayed a fast ( $\approx 1.1$  s) and ultrasensitive response (1% water adsorption corresponds to a 0.69% decrease in the PL intensity) to humidity in a broad operation range (i.e., from 10% to 90% RH). As a proof of concept, the authors deposited these elastomers on a hydrophilic and porous cellulose acetate nanofiber by a simple dip-coating process for real-time and reversible monitoring of environmental humidity and human respiration.<sup>[19]</sup>

A structurally simpler yet extremely sensitive optical sensor was reported by Squillaci et al.<sup>[18]</sup> where 2D networks of AuNPs, interconnected with moisture-responsive hygroscopic organic linkers (e.g., 7 nm long dithiolated poly(ethylene glycol) (PEG) molecules) were fabricated (Figure 3c). The smart design of these supramolecular nanostructures was based on the multiple roles played by the dithiolated poly(ethylene glycol) linkers. Firstly, the presence of two thiol groups in their structure enabled them to strongly interact with AuNPs, allowing the formation of a 2D network of AuNPs with fine control of the interparticle distance. Secondly, due to the hygroscopic nature of the poly(ethylene glycol) backbone, it guaranteed strong affinity to moisture. Single noble-metal NPs exhibit distinct optical properties arising from their localized surface plasmon resonance

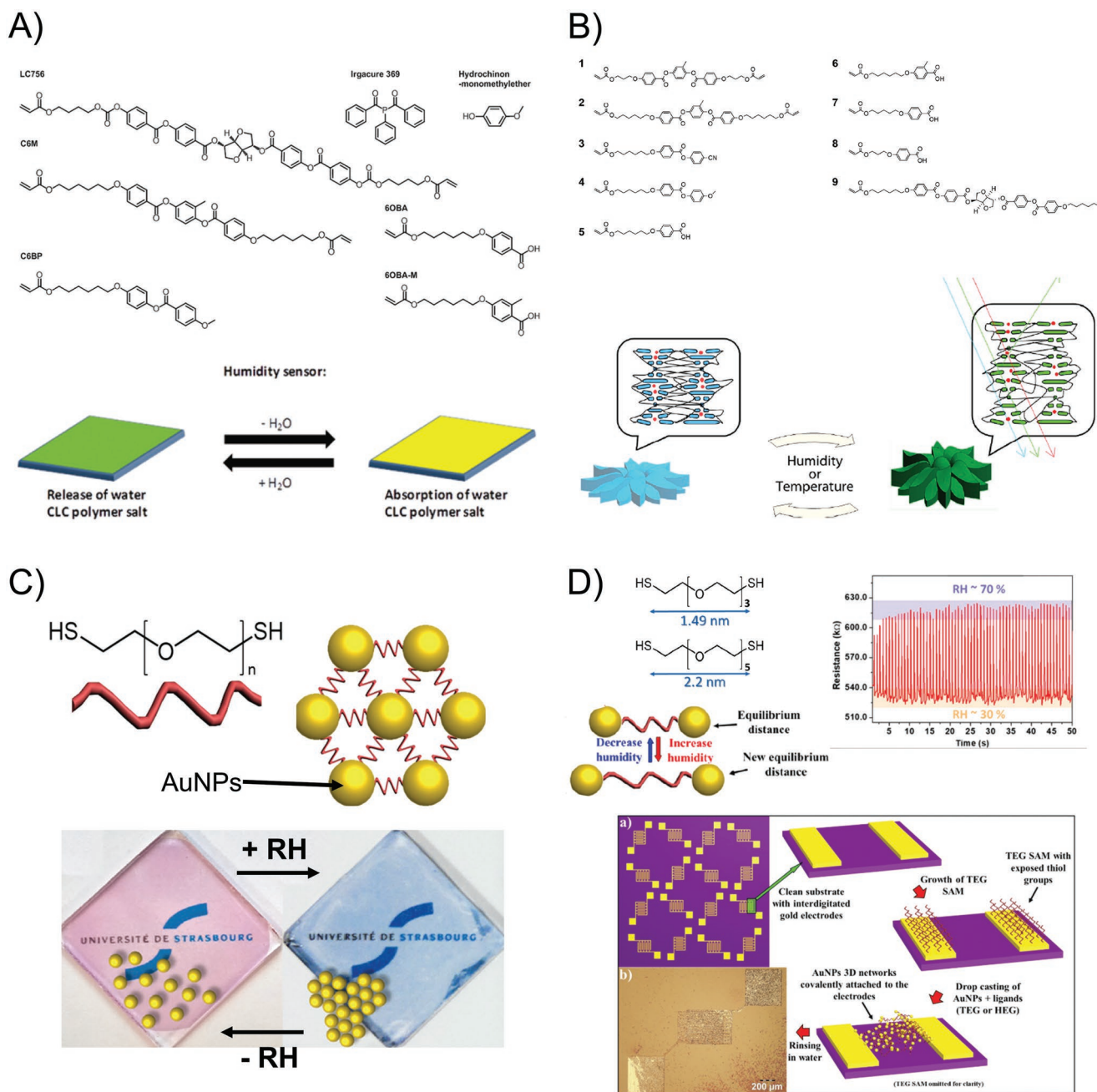


**Figure 3.** Supramolecular humidity sensors with swelling sensing mechanism. A) Top: Chemical composition of the CLC mixture. Bottom: Schematic representation of the humidity sensor. A) Reproduced with permission.<sup>[25]</sup> Copyright 2012, American Chemical Society. B) Top: Chemical composition of the CLC mixture. Bottom: Schematic representation of the moisture and temperature responsive microactuator. B) Reproduced with permission.<sup>[21]</sup> Copyright 2020, American Chemical Society. C) Top: Crosslinking reaction of AuNPs with dithiolated PEG into 2D networks. Bottom: Effect of humidity on the macroscopic optical properties of 2D AuNP/PEG networks. C) Reproduced with permission.<sup>[18]</sup> Copyright 2019, Royal Society of Chemistry. D) Top left: Molecular structure and corresponding nominal fully elongated length of dithiolated TEG (4 repetitive units) and HEG (6 repetitive units). Top right: Device's response to short pulses of humid air (RH  $\approx$  70%) under ambient conditions (constant bias applied = 500 mV). Bottom: Optimized procedure for the fabrication of 3D AuNPs-TEG based electrical devices. D) Reproduced with permission.<sup>[24a]</sup> Copyright 2019, Royal Society of Chemistry.

(LSPR), which depends not only on their composition, size and shape but also on the refractive index of their environment. When the distance between noble-metal NPs decreases (i.e., with a spacing of a few nanometers), a coupling of the LSPR takes place, dramatically modifying the optical properties and therefore resulting in a color change easily visible by the naked

eye in some cases. Colorimetric sensors based on noble-metal NPs, specially AuNPs, have been extensively used due to their simplicity, cost-effectiveness, quickness, and unprecedented selectivity among the traditional detection methodologies. When AuNPs/dithiolated PEG 2D all-covalent networks were exposed to humidity, water molecules can undergo reversible

**Table 1.** Supramolecular nanostructures for humidity sensing and their respective KPIs.

Receptor	Sensing strategy	Working range [%RH]	Sensitivity	Interfering compounds	Temperature calibration	Response time	Recovery time	Reference
<b>Morphological and structural changes</b>								
<b>Swelling mechanism</b>								
Cholesteric liquid crystal <sup>a)</sup>	Colorimetric	3–83	–	–	No	2 min	3 min	Ref. [25]
Cholesteric liquid crystal <sup>b)</sup>	Optical	42–75	–	–	Yes	≈12 s	≈3 s	Ref. [21]
Polyurethane ether glycol	Fluorescence	10–90	0.069 <sup>Lfd)</sup>	–	No	1.1 s	5.7 s	Ref. [19]
Tetraethylene glycol or hexaethylene glycol	Chemiresistor	5–85	–	–	Yes	≈26 ms	≈250 ms	Ref. [18]
Polyethylene glycol	Colorimetric	11–94	51 kΩ per RH [%]	–	No	200 ms	–	Ref. [24a]
<b>Shrinking mechanism</b>								
Coronene tetracarboxylate salt and dodecyl methyl viologen	Chemiresistor	5–85	10 <sup>4</sup> Ne)	–	No	8 ms	24 ms	Ref. [33]
Coronene tetracarboxylate salt and dodecyl methyl viologen	Chemiresistor	5–70	–	–	No	–	Moisture memory device	Ref. [20]
Tetrathiophene and a perylene <sup>di</sup> imide	Chemiresistor	0–75	10 <sup>7</sup> N	Ethanol, methanol, and ethyl ether	No	26 ms	–	Ref. [34]
Oligoethylene glycol benzothienobenzothiophene	Chemiresistor	10–80	10 <sup>2</sup> N	–	No	≈100–500 ms	≈100–500 ms	Ref. [26]
Naphthalimide-based compounds <sup>c)</sup> and α-cyclodextrin	Fluorescence	40–70	–	–	No	43–105 min	–	Ref. [35]
<b>Charge-transport changes</b>								
<b>Proton/ion-transport mechanism</b>								
Prnctide halides: (Hg <sub>9.75</sub> As <sub>5.5</sub> )(GaCl <sub>4</sub> ) <sub>3</sub> or (Hg <sub>13</sub> Sb <sub>8</sub> )(ZnBr <sub>4</sub> )	Chemiresistor	3–93	10 <sup>3</sup> N	–	No	20 or 1 s	24 or 3 s	Ref. [36]
Prnctidehalide (Hg <sub>6</sub> P <sub>4</sub> )(CrCl <sub>6</sub> )Cl	Chemiresistor	10–90	10 <sup>4</sup> N	–	No	162 s	15 s	Ref. [38]
[(Cd <sub>0.5</sub> (cfH)(4,4'-bpy) <sub>0.5</sub> )(NO <sub>3</sub> )·H <sub>2</sub> O] <sub>n</sub> (named as CdL, cfH = ciprofloxacin, 4,4'-bpy = 4,4'-bipyridine)	Chemiresistor	11–97	3.15 10 <sup>3</sup> N	–	No	12 s	53 s	Ref. [24b]
[Pb(TMA)] <sub>n</sub> (noted as PbL, H <sub>2</sub> TMA = 3-thiophenemalonic acid)	Chemiresistor	11–97	3.1 10 <sup>2</sup> N	–	No	9 s	38 s	Ref. [29a]
Pyranine	Chemiresistor	11–95	–	–	No	2 s	6 s	Ref. [23]
<b>Electron-transport mechanism</b>								
Py-TT COF: 1,3,6,8-tetrakis(4-aminophenyl)pyrene, and thieno-[3,2-b]thiophene-2,5-dicarboxaldehyde	Colorimetric	0.59–0.98 H <sub>2</sub> O partial pressure (p/p <sub>0</sub> )	–	Methanol, ethanol, acetonitrile, toluene, hexane	No	110 ms	90 ms	Ref. [27b]
Aniline	Chemiresistor	10–90	–	Ar, O <sub>2</sub> , N <sub>2</sub> , CO <sub>2</sub>	No	≈50 ms	≈50 ms	Ref. [22]
2-[2-(2-Methoxyethoxy)-ethoxy]ethylamine	Chemiresistor	2–97	31% N	Methanol, ethanol, acetone, chloroform	No	25 ms	127 ms	Ref. [27a]
Perovskite/zeolite composite, Cs <sub>4</sub> PbBr <sub>6</sub> /FAU-Y	Fluorescence	0.56–98	992 N	–	–	–	–	Ref. [41]
<b>Electron/proton mixed transport mechanism</b>								
2,2'-Azino-bis(3-ethylbenzothiazoline-6-sulfonic acid) and 1,10-Bis(3-methylimidazolium-1-yl)decane	Chemiresistor	0-86	–	N <sub>2</sub> , CO <sub>2</sub> , O <sub>2</sub>	No	≈37 ms	85 ms	Ref. [15b]
Benzothienobenzothiophene and methyl-terminated diethylene glycol	Chemiresistor	10–80	10 <sup>3</sup> N	Methanol, ethanol, diethyl ether	No	≈100–500 ms	≈100–500 ms	Ref. [13]

Table 1. continued.

Receptor	Sensing strategy	Working range [%RH]	Sensitivity	Interfering compounds	Temperature calibration	Response time	Recovery time	Reference
<b>Hybrid mechanism</b>								
Poly(vinyl alcohol)	Chemiresistor	40–100	58.3% $\Delta$ RH	–	No	10 min	–	Ref. [32]
Poly(diallylimethylammonium chloride)	Chemiresistor	11–97	0.32 <sup>LF</sup>	–	No	300 s	200 s	Ref. [30a]
Azobenzene dicarboxylate and cetyltrimethylammonium bromide	Chemiresistor	10–70	–	–	Yes	–	–	Ref. [30b]
Poly(vinylpyrrolidone) and <i>N,N</i> -diethyl-4-((4-nitrophenyl)diazenyl)aniline or 2-(ethyl(4-((4-nitrophenyl)diazenyl)phenyl)amino)ethan-1-ol	Colorimetric	50–75	–	N <sub>2</sub> , CO <sub>2</sub>	No	5 s	Moisture memory device	Ref. [28]
4-((2,2'':6'',2''-terpyridin)-4'-yl)phenyl)pyridine-2,6-dicarboxylic acid	Fluorescence, chemiresistor	60–100 25–100	–	–	Yes	–	–	Ref. [29b]

<sup>a)</sup> (3R,3aS,6R,6aS)-6-(((4-(((4-(Acryloyloxy)butoxy)carbonyl)oxy)benzoyl)oxy)benzoyl)oxy)hexahydrofuro[3,2-b]furan-3-yl 4-(((4-(acryloyloxy)butoxy)carbonyl)oxy)benzoate (**LC756**) + 2-methyl-1,4-phenylene bis(4-(((6-(acryloyloxy)hexyl)oxy)carbonyl)oxy)benzoate (**C6M**) + 4-(((6-(acryloyloxy)hexyl)oxy)phenyl 4-methoxybenzoate (**C6BP**) + 4-(((6-(acryloyloxy)hexyl)oxy)benzoic acid-methane (1/1) (**6OBA**) + 4-(((6-(acryloyloxy)hexyl)oxy)-2-methylbenzoic acid-methane (1/1) (**6OBA-M**) + (phenylphosphonediyl)bis(phenylmethanone) (**Irgacure 369**) + hydroquinon-monomethylether; <sup>b)</sup> 2-Methyl-1,4-phenylene bis(4-(3-(acryloyloxy)propoxy)benzoate), 2-methyl-1,4-phenylene bis(4-(((6-(acryloyloxy)hexyl)oxy)benzoate), 4-cyanophenyl 4-(((6-(acryloyloxy)hexyl)oxy)benzoate, 4-methoxyphenyl 4-(((6-(acryloyloxy)hexyl)oxy)benzoate, 4-(((6-(Acryloyloxy)hexyl)oxy)benzoic acid, 4-(((6-(acryloyloxy)hexyl)oxy)-2-methylbenzoic acid, 4-(((5-(acryloyloxy)pentyl)oxy)benzoic acid, 4-(3-(acryloyloxy)propoxy)benzoic acid; <sup>c)</sup> (8S,9S,10R,13R,14S,17R)-10,13-Dimethyl-17-((R)-6-methylheptan-2-yl)-2,3,4,7,8,9,10,11,12,13,14,15,16,17-tetradecahydro-1H-cyclopenta[a]phenanthren-3-yl (2-(6-(6-((2-(adamantane-2-carboxamido)ethyl)amino)-1,3-dioxo-1H-benzo[de]isoquinolin-2(3H)-yl)hexanamido)ethyl)carbamate and (8S,9S,10R,13R,14S,17R)-10,13-dimethyl-17-((R)-6-methylheptan-2-yl)-2,3,4,7,8,9,10,11,12,13,14,15,16,17-tetradecahydro-1H-cyclopenta[a]phenanthren-3-yl (2-(6-(1,3-dioxo-6-((2-(2,3,4,5,6-pentahydroxyhexanamido)ethyl)amino)-1H-benzo[de]isoquinolin-2(3H)-yl)hexanamido)ethyl)carbamate; <sup>d)</sup> LF: Linear fitting; <sup>e)</sup> N: Normalized (e.g., ratio between the output signal at high and low RH %).

adsorption/desorption within the PEG backbone, determining a swelling/shrinking of the latter macromolecule and dynamically modifying the interparticle distance, thus their LSPR coupling. A fully reversible sensing process characterized by a response speed of 200 ms and stability over hundreds of cycles was achieved for the first time by using the dynamic water physical adsorption–desorption and the use of dithiolated linkers. By controlling the humidity level (i.e., 0–97% RH) the authors were able to tune the interparticle distance achieving a maximum shift of the LSPR band as large as 35 nm in the visible range (from a dry state to complete immersion in water) which can be detected by naked eye.<sup>[18]</sup>

Upon using shorter, thus conformationally stiffer, dithiolated PEG oligomers, Squillaci et al.<sup>[24a]</sup> reported the fabrication of electrical humidity sensors based on 3D porous networks of dithiolated PEG / AuNPs (Figure 3d). This self-assembled system was composed of AuNPs operating as the electrical transducing elements and PEG, acting as the sensing element as well as ensuring the charge transport via direct tunneling. Upon interaction with water molecules, the 3D networks underwent swelling, the interparticle distance increased and therefore the tunneling current passing through the system was proportionally reduced. The authors studied the effect of two dithiolated ethylene glycol with different chain lengths, comprising 4 (TEG) or 6 (HEG) ethylene glycol repetitive units and demonstrated that such a small difference in the backbone chain length (nominally 0.7 nm) yielded a dramatic and predictable difference of the device performances to meet different application requirements. TEG-based devices exhibited an unprecedentedly high response and recovery time ( $\approx$ 26 and  $\approx$ 250 ms, respectively), no hysteresis effect nor fatigue effect over hundreds of water adsorption/desorption cycles, and a

linear response to humidity changes (0–100% RH) characterized by a high sensitivity of 500  $\Omega$  per RH (%).<sup>[24a]</sup>

### 5.1.2. Shrinking Mechanism

The opposite mechanism to swelling is shrinking mechanism, where the adsorption of water into the structure of the sensing element triggers a contraction of the nanoporous material when the relative humidity increases. These changes were monitored as well by both optical and electrical readout.

Donor–acceptor (D–A) dyads are well-known molecular systems that can undergo self-assembly forming fibers that exhibit good (photo)electrical characteristics. For instance, Mogera et al.<sup>[33]</sup> reported an ultrafast (<10 ms), wide operation range (5–85% RH), highly sensitive (<10<sup>4</sup>) and highly stable (lifecycle > 8 months) resistive humidity sensor based on donor and acceptor molecules (i.e., coronene tetracarboxylate (CS) and dodecyl methyl viologen (DMV) respectively), self-assembled into supramolecular nanofibers (Figure 4a). The  $\pi$ – $\pi$  interaction between the donor and the acceptor molecules depends sensitively on the surrounding humidity, influencing electrical conduction across the nanofiber. When these nanofibers were exposed to an increasing amount of humidity, the system conductivity simultaneously increases. The authors proved via ultraviolet–visible (UV–vis), powder X-ray diffraction (PXRD) and atomic force microscope (AFM) measurements that with the increase in RH, the stacking distance in the nanofiber decreased slightly while the charge-transfer band intensity increased, all observations implying enhanced charge-transfer interaction and hence the conductivity. As proof of concept, the authors demonstrated the potential applications in personal



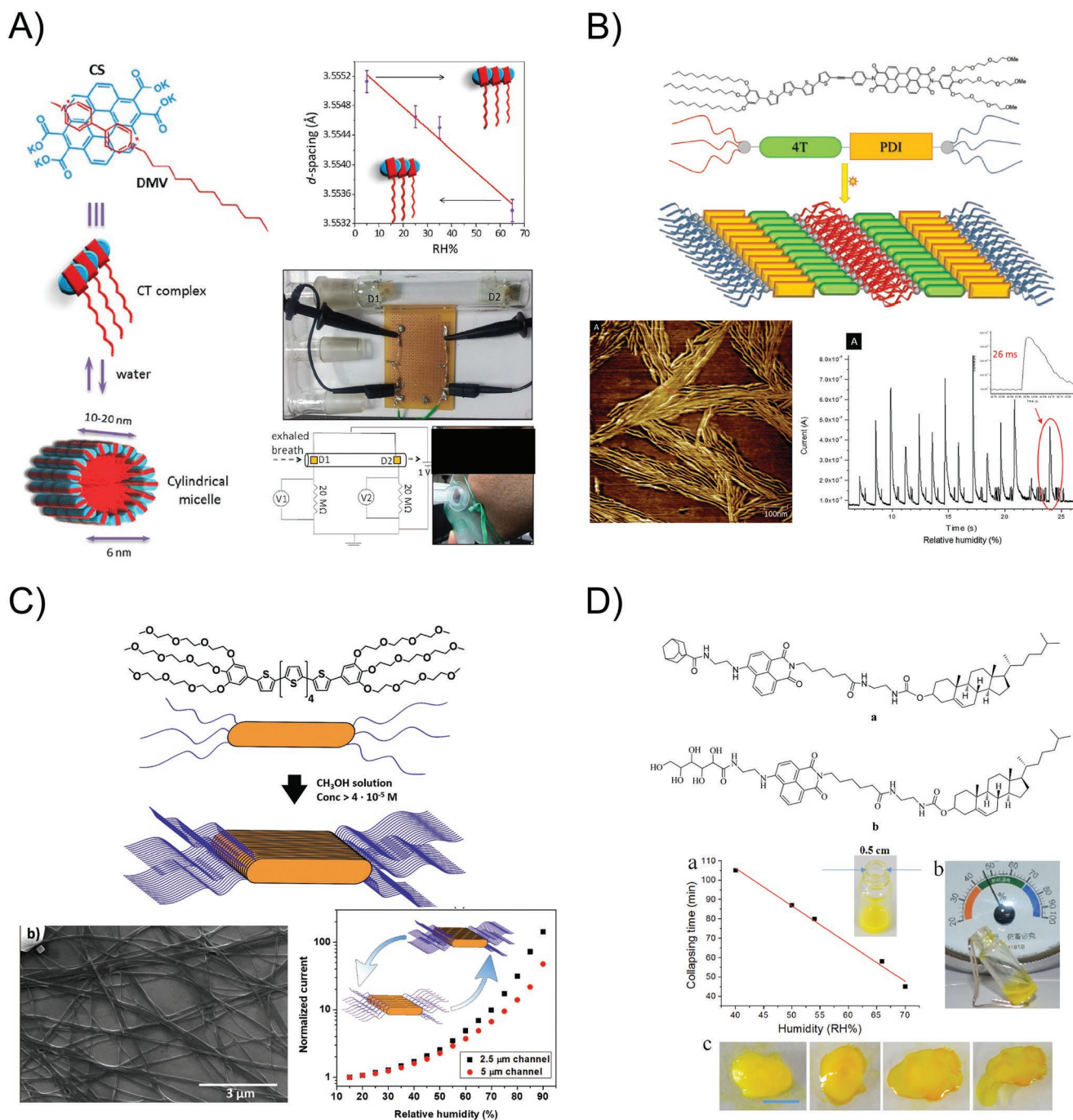


**Figure 4.** Supramolecular humidity sensors with shrinking sensing mechanism. A) Left: Molecular structure and schematic of the charge-transfer complex involving cofacial arrangement of the aromatic donor, CS and the acceptor, DMV. Top right: The variation in the PXRD *d*-spacing with RH. Bottom right: A photograph of the humidity, the circuit diagram of the experimental set up is shown below and a photograph of a volunteer performing breathing trial. A) Adapted with permission.<sup>[33]</sup> Copyright 2014, The Authors, published by Springer Nature. (Ref. [33] is originally published under a Creative Commons Attribution-NonCommercial-NoDerivs 3.0 Unported license) B) Top: Molecular structure and packing model of PDI-4T dyad. Bottom left: AFM phase image of PDI-4T nanoribbons on SiO<sub>2</sub> substrate. Bottom right: Response speed under a pulsed flow of humid air during the application of a constant bias of 5 V (channel length = 5 μm). B) Reproduced with permission.<sup>[34]</sup> Copyright 2015, Wiley-VCH. C) Top: Molecular structure of OT-TEG and proposed self-assembly into 1D structures in methanol solution. Bottom left: SEM image of OT-TEG. Bottom right: Normalized calibration curves for interdigitated devices with 2.5 and 5 μm channel lengths. c) Reproduced with permission.<sup>[26]</sup> Copyright 2018, Wiley-VCH. D) Top: Chemical structures of the amide derivatives. Bottom: Linear relationship of the gel collapsing time as a function of RH at 25 °C (a); photograph of the hygrometer STH310 used in the test (b); and from left to right: photographs of the gel kept at 54% RH after 10, 20, 30, and 43 min; scale bar: 1 cm (c). D) Reproduced with permission.<sup>[35]</sup> Copyright 2017, American Chemical Society.

healthcare as use-and-dispose devices for dynamic monitoring of human breath. Using two humidity sensors, a breath flow sensor was fabricated which allowed the simultaneous measurement of RH and the flow rate of exhaled nasal breath.<sup>[33]</sup>

By mastering the donor–acceptor approach, the same authors reported the fabrication of a humidity-responsive device that displayed a moisture memory effect.<sup>[20]</sup> The device was based on the same supramolecular nanofibers obtained from the self-assembly of D–A molecules, CS and DMV, respectively. The assembly and associated conductivity of the resulting fibers were very sensitive to external stimuli (i.e., humidity and electric field) with the combination leading to an efficient humidity memory sensor. The authors found that when the fibers were under continued electrical stress while applying multiple RH pulses, steady decay in the conductivity through the fibers was observed due to increasing disorder in the molecular assembly. The initial state can be recovered by exposing the device to humidity in the absence of applied voltage. Interestingly, the humidity memory state was independent of the lapsed time since the humidity exposure as well as the duration of exposure and the device was capable of differentiating the profiles of varying humidity conditions from its memory.<sup>[20]</sup>

Another example was reported by Squillaci et al.<sup>[34]</sup> where white light-irradiation triggered the self-assembly of an electron D–A dyad, based on a conjugated backbone containing tetrathiophene and perylenediimide connected by a conformationally rigid ethynylene spacer (PDI-4T) (Figure 4b). These conjugated molecules were amphiphilic as they exposed lateral ethylene glycol and alkyl chains. The supramolecular fibers produced by molecular self-assembly were decorated by an external moisture responsive ethylene glycol shell. Such fibers were employed as active components in resistive humidity sensors, exhibiting high sensitivity and ultrafast response (i.e., 26 ms). Analogously to Mogera et al. work,<sup>[33]</sup> the authors observed an increase in the conductivity of its system proportional to the RH level, which they attributed to the decrease in the  $\pi$ – $\pi$  stacking distances with the increasing humidity level.<sup>[34]</sup>

More recently, the same authors reported the design and synthesis of a structurally simpler, new symmetric oligothiophene exposing TEG-based side-chains (OT-TEG) (Figure 4c).<sup>[26]</sup> In solution the conjugated oligothiophene backbones were phase segregated on the sub-nanometer scale from the TEG side-groups, forming  $\pi$ – $\pi$  stacked conductive supramolecular fibers coated by a hygroscopic shell which displayed a certain affinity for polar molecules. Upon exposure to humidity, such supramolecular architectures were capable of reversibly adsorbing and desorbing water molecules within the hygroscopic TEG branches. The adsorption of water caused a fast (i.e., 45 ms) and reproducible increase of the electrical current through the fibers by a factor of 100 from 15% to 90% RH, as measured in 2-terminal devices. The adsorbed water molecules acted as a bridge between intermolecular TEG chains, using H-bonding to disrupt the electrostatic repulsion, ultimately improving the packing within the fibers and decreasing the intermolecular  $\pi$ – $\pi$  distance. Such subtle structural modifications had a dramatic impact on the transfer integral and therefore on the electrical current passing through the fibers via intermolecular hopping.<sup>[26]</sup>

A different approach was employed by Yu et al.<sup>[35]</sup> by fabricating a two-component gel as a visual humidity sensor (Figure 4d). The stimuli-responsive gel was formed via the fast interaction of  $\alpha$ -cyclodextrin ( $\alpha$ -CD) (as a proton donor) with an amide derivative (as a proton acceptor), triggered by ultrasounds. The  $\alpha$ -CD acted as a junction for the assembly of the naphthalimide-based compounds through hydrogen bonding between hydroxyl and amide groups. Upon addition of water,  $\alpha$ -CD interacted with the adamantane group of amide derivative via an incomplete host–guest encapsulation, resulting in the dissociation of the hydrogen-bonding-assisted two-component assembly, accompanied by a visual gel collapse.<sup>[35]</sup>

The majority of optical humidity sensors based on supramolecular nanostructures are governed by morphological and structural changes as the swelling or shrinking of the nanostructures is usually accompanied by a macroscopic color change, easily detectable by the naked eye. However, most of optical sensors usually display a lower responsiveness (i.e., longer response and recovery time) than electrical humidity sensors. Among the different supramolecular receptors, ethylene glycol units have shown the broadest operation ranges (5–94% RH) as well as the highest responsiveness, together with coronene tetracarboxylate salt and dodecyl methyl viologen and a tetrathiophene–perylene diimide dyad (8–200 ms as both response and recovery time). In particular, the tetrathiophene–perylene diimide dyad displayed the highest sensitivity among all the reported supramolecular humidity sensors, up to seven orders of magnitude of difference between the output signal at lowest and highest humidity level.

## 5.2. Charge-Transport Changes

A different process taking place when water interacts with the supramolecular nanostructures consists in changes in the ability of specific materials to transport or accumulate charges (electronic or ionic species). In this framework, humidity-responsive materials and devices can be designed and optimized to feature high performance via the in-depth understanding of the influence of the adsorbed water on such electronic/ionic conduction processes.

### 5.2.1. Proton/Ion-Transport Mechanism

This mechanism was solely exploited, to the best of our knowledge, by means of electrical readout. The adsorption of water into the structure of the sensing element triggers an increase in the conductivity of the system, or in other words a decrease of resistance or impedance.

Metal pnictide halides, which usually combine metal pnictide frameworks with positive charges as hosts and metal halide polyanions as guests, are an important subgroup of supramolecular host–guest complexes (HGCs). Two novel metal pnictide halides,  $(\text{Hg}_{9,75}\text{As}_{5,5})(\text{GaCl}_4)_3$  (1) and  $(\text{Hg}_{13}\text{Sb}_8)(\text{ZnBr}_4)$  (2), have been prepared by solid-state reactions and their performance as chemiresistive humidity sensors was assessed by Jian et al.<sup>[36]</sup> The resistances for single crystals of 1 and 2 as a function of RH and dynamic response measurements indicated

that both compounds exhibited good single-crystal humidity sensitivity, with a humidity sensitivity factor as big as three orders of magnitude, a quick resistance response (i.e., 20 or 1 s, respectively), a fast recovery (i.e., 24 or 3 s, respectively), and good reproducibility. The adsorption and desorption of water molecules on the crystal surfaces of 1 and 2 were reversible, clearly indicating weak van der Waals interactions between the adsorbed water molecules and their surfaces. The channels of the host frameworks were filled with anionic guests and therefore water molecules can barely enter into the crystals. The large decrease in resistance with higher RH in both compounds was ascribed to the ionic conductance of  $\text{H}^+$  or  $\text{H}_3\text{O}^+$  in the adsorbed water layers formed on the surfaces.<sup>[37]</sup> At low humidity, where only a few water molecules were adsorbed, the ionic conduction was weak and the resistance was relatively high. Upon increasing the environmental humidity, continuous water layers can be formed on the crystal surfaces, which accelerated the transfer of  $\text{H}^+$  or  $\text{H}_3\text{O}^+$  ultimately leading to a rapid decrease in resistance.<sup>[36]</sup>

Following a similar approach, Peng et al.<sup>[38]</sup> reported the synthesis of a new metal pnictidehalide  $(\text{Hg}_6\text{P}_4)(\text{CrCl}_6)\text{Cl}$  by solid-state reaction.<sup>[38]</sup> Its structure featured a 3D perovskite-like  $3_6(\text{Hg}_6\text{P}_4)^{4+}$  host octahedral network and discrete octahedral  $(\text{CrCl}_6)^{3-}$  and  $\text{Cl}^-$  guest ions assembled by weak van der Waals interactions. This complex was assessed as a resistive humidity sensor exhibiting high sensitivity (i.e., up to four orders of magnitude of resistance difference between 10% and 90% RH), quick response (i.e., 162 s), fast recovery (i.e., 15 s), and good reproducibility (i.e., when the sensor was exposed to 70% RH, the current reverts to the original value when RH was restored to 10% RH). Similar to Jian et al.,<sup>[36]</sup> the authors observed an increase in the current of the system with the increase in humidity. As water molecules cannot penetrate into the pnictidehalide structure due to the presence of anionic species, the moisture–material interactions were ascribed to the same mechanism of ionic conduction promoted by the adsorbed water molecules on the pnictidehalide surface.<sup>[38]</sup>

Coordination polymers (CPs), metal–organic frameworks (MOFs) and covalent organic frameworks (COFs) hold great potential as humidity sensors, not only because of their good structural tunability and easy processability but also due to their abundant pores, as well as their high specific surface area. For instance, Li et al.<sup>[24b]</sup> reported the synthesis of a 1D Cd(II) coordination polymer,  $([\text{Cd}_{0.5}(\text{cfH})(4, 4'\text{-bpy})_{0.5}](\text{NO}_3) \cdot \text{H}_2\text{O})_n$  (named as CdL, cfH = ciprofloxacin, 4,4'-bpy = 4,4'-bipyridine), via a facile solvent evaporation method at room temperature (Figure 5a).<sup>[24b]</sup> Furthermore, the chains of this polymer were further connected by hydrogen bonds forming a 3D supramolecular network. The CdL impedimetric humidity sensor, operating at an alternating current (AC) voltage and frequency of 1 V and 100 Hz, respectively, exhibited high sensitivity (i.e., impedance changes higher than three orders of magnitude from 11% to 97% RH), small hysteresis, and short response–recovery times (i.e., 12 and 53 s, respectively). Importantly, the authors shed light onto the sensing mechanism by analyzing the Nyquist plots in the frequency range of 50 Hz to 100 kHz. Three different regimes were found: i)  $\text{RH} < 54\%$ , ii)  $54\% < \text{RH} < 85\%$ , and iii)  $85\% < \text{RH} < 97\%$ . At low RH range (11–54%), only a few water molecules were captured

by CdL surface forming a discontinuous water coverage. The impedance was an arc of a semicircle and large impedance values (hundreds of  $\text{M}\Omega$ ) were recorded because the electrolytic conduction ( $\text{H}_2\text{O} \rightarrow \text{H}^+ + \text{OH}^-$ ) is difficult to happen in this stage.<sup>[24b]</sup> With the increase of RH (54–85%), the arc grew to be a semicircle, and the radius of which became gradually smaller. The increase in the number of water molecules physically adsorbed onto the CdL surface led to the formation of a continuous liquid-like layer. In this layer, water molecules can be ionized with the help of an electric field, generating moveable proton ( $\text{H}^+$ ) and hydronium ions ( $\text{H}_3\text{O}^+$ ). According to the protons conductivity model,  $\text{H}_3\text{O}^+$  is more stable than  $\text{H}^+$  and therefore  $\text{H}_3\text{O}^+$  will be the dominant charge carrier in this stage. These charge carriers significantly reduce the impedance based on the ion-transfer mechanism of the Grotthuss reaction:  $\text{H}_2\text{O} + \text{H}_3\text{O}^+ \rightarrow \text{H}_3\text{O}^+ + \text{H}_2\text{O}$ , ensuring the easy movement of  $\text{H}_3\text{O}^+$  in the continuous water layer under alternating electric fields.<sup>[39]</sup> At 97% RH, a straight line emerged attached to the semicircle in the low-frequency range (right half part in a Nyquist plot), indicating the impact of  $\text{H}_3\text{O}^+$  in the physically adsorbed water layer through  $\text{H}^+$  jumping between adjacent water molecules. Based on complex impedance spectra analysis, the sensing mechanism of this CdL sensor indicated the significant roles played by distinct charge carriers at different RH ranges.<sup>[24b]</sup>

In parallel, Yin et al.<sup>[29a]</sup> reported the synthesis and fabrication of a 2D honeycomb-layered topological coordination polymer with the formula of  $[\text{Pb}(\text{TMA})]_n$  (noted as PbL,  $\text{H}_2\text{TMA}$  = 3-thiophenemalonic acid) as an impedimetric humidity sensor. The PbL consisted of a 6, 3-connected network with thiophene rings on each side of the honeycomb layer. Importantly, the unusual short bond of Pb–S (3.39 Å) allowed the generation of a 3D supramolecular framework. Based on the abundant active sites (such as  $\text{Pb}^{2+}$  ions, O and S atoms), promoting the adsorption and interaction of water molecules on the PbL surface, an impedimetric humidity sensor was fabricated.<sup>[29a]</sup> The authors investigated the dependence of impedance on the RH for PbL at a frequency ranging from 10 Hz to 100 kHz. While the impedance values decreased gradually with the increased of RH, the highest sensitivity was obtained in the low-frequency region of 10–100 Hz. The PbL sensor exhibited a highly sensitive response (i.e., up to two orders of magnitude of impedance change between 11% and 97% RH), good repeatability, small hysteresis, as well as short response and recovery times (i.e., 9 and 38 s, respectively). Analogously to Li et al. work,<sup>[24b]</sup> the authors explained the sensing mechanism by analyzing the Nyquist plots in the frequency range of 10 Hz to 100 kHz, finding two different regimes: i)  $11\% < \text{RH} < 54\%$ , ii)  $54\% < \text{RH} < 97\%$ . The distinct charge carriers in each regime were analogous to the previous case.<sup>[24b,29a]</sup>

Pristine graphene oxide (GO) and reduced graphene oxide (rGO) are 2D materials that have been applied in different fields, including energy storage systems, water purification and wearable electronics. GO has been exploited in humidity and temperature sensors displaying a number of convenient features such as flexibility, transparency and suitability for large-scale manufacturing. For instance, Borini et al.,<sup>[40]</sup> reported an impedimetric humidity sensor by solely using GO as sensing material and due to its wettability, an unprecedented response

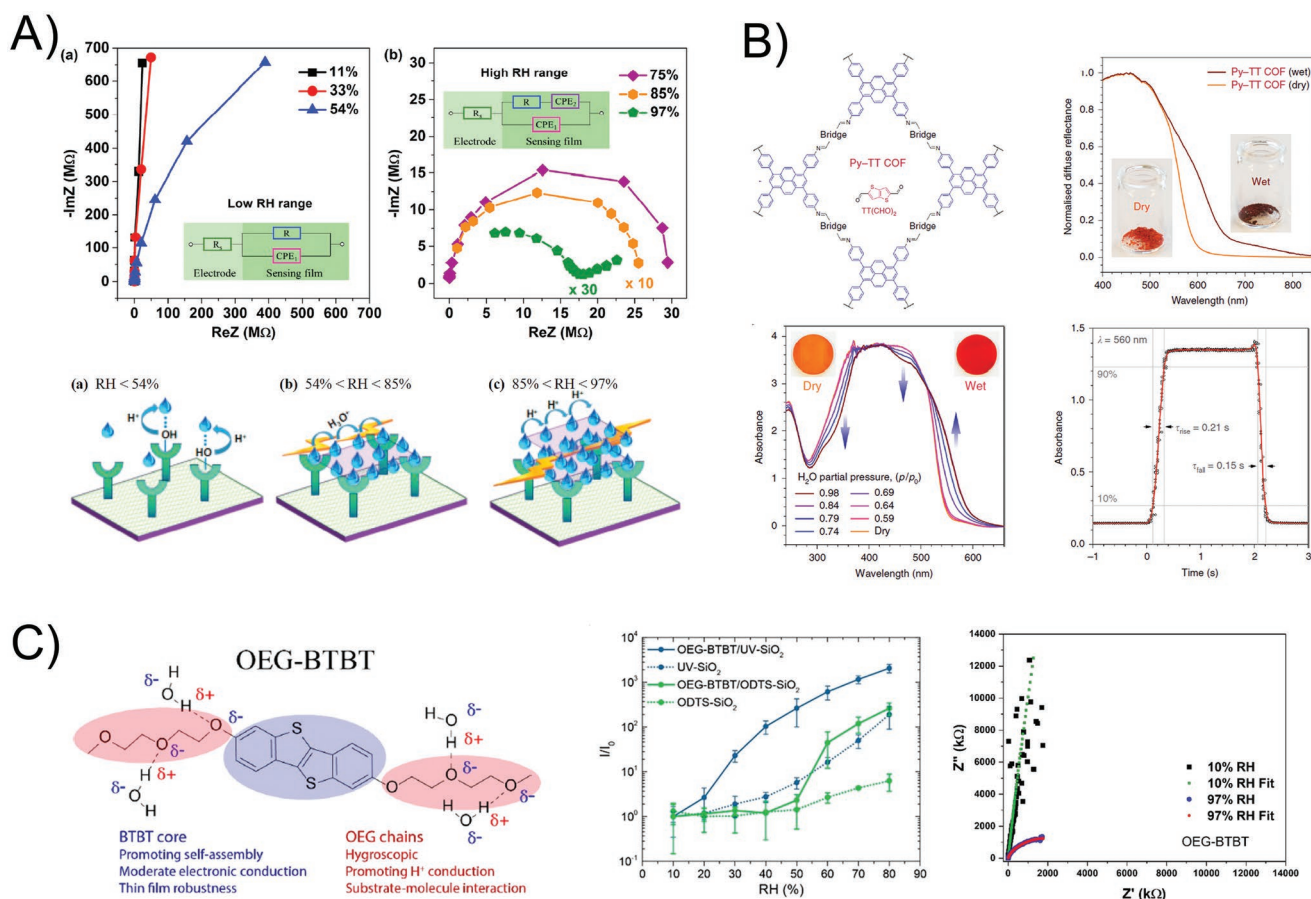


**Figure 5.** A) Supramolecular humidity sensors with proton/ion-transport sensing mechanism. a, b) Complex impedance property of the CdL sensor at various RH ranges: a) 11–54%, and b) 75–97%. Inset: Top: the equivalent circuits of complex impedance plots at low RH (11–54%) (a) and high (b) RH (75–97%). Bottom: The proposed humidity sensing mechanism of the CdL based sensor under different RH ranges (bottom). A) Reproduced with permission.<sup>[24b]</sup> Copyright 2019, Elsevier. b) Top left: Electron-transport sensing mechanism. Py-TT COF structure. Top right: Diffuse reflectance spectra of the dry (orange) and water vapor-saturated (brown) Py-TT COF powder showing a strong solvatochromic redshift. Bottom left: UV-vis absorption spectra of the Py-TT COF film recorded at different relative pressures of  $H_2O$  in  $N_2$ . Bottom right: Solvatochromic response of the Py-TT COF film toward step changes between dry and  $H_2O$ -saturated  $N_2$  streams. B) Reproduced under the terms of the CC-BY Creative Commons Attribution 4.0 International license (<https://creativecommons.org/licenses/by/4.0>).<sup>[27b]</sup> Copyright 2018, The Authors, published by Springer Nature. C) Electron/proton mixed transport sensing mechanism. Top: Chemical structure of the OEG-BTBT molecule and its interaction with atmospheric water molecules via H-bonding interactions. Bottom left: Current response of OEG-BTBT devices fabricated on treated  $SiO_2$  (UV/ozone and ODTS, solid lines) and bare substrates (dotted lines). Bottom right: Nyquist plot for OEG-BTBT thin-film two-terminal devices at low (10%) and high (97%) RH. C) Reproduced with permission.<sup>[13]</sup> Copyright 2022, American Chemical Society.

speed ( $\approx 30$  ms response and recovery times) was achieved. The high sensitivity of electrochemical impedance spectroscopy (EIS), is convenient for samples with low conductivity, such as GO. However, EIS is not suitable for practical applications as it is sensitive to the surrounding environment, often requires a Faraday cage to reduce noise, bulky experimental setups and the need for theoretical simulation for data analysis. Although it is highly conductive, due to its hydrophobic character, pristine rGO is not useful when applied as humidity sensors, since it exhibits slow response and recovery as well as low sensitivity toward gas or humidity changes. Fortunately, this problem can be overcome with proper chemical functionalization. For instance, Chen et al. reported a facile one-step supramolecular assembly method to functionalized rGO with the organic molecule pyranine (Pyr-rGO) for achieving a remarkable humidity sensing performance.<sup>[23]</sup> The imped-

metric humidity sensor based on Pyr-rGO exhibited a highly sensitive response (i.e., impedance ratio at 11% and 95% RH of 6000), fast response and recovery time (i.e., 2 and 6 s), small hysteresis of 8% RH; reliable repeatability and excellent life-cycle (i.e., over 100 cycles). Importantly, the authors provided a detailed mechanism analysis of the moisture-material interactions based on impedance spectroscopy to investigate the difference in water adsorption and ions transfer under various RH levels. Three different regimes were found: i) 11% < RH < 33%, ii) 34% < RH < 74%, and iii) 75% < RH < 95%. At low RH range (11–33% RH), the Nyquist plots showed almost straight lines. Similar to the previously described mechanism, at this low RH range, chemical adsorption was the main adsorption method in humidity sensing, where only a few water molecules can be adsorbed onto the surface of Pyr-rGO film. After the chemical adsorption, a proton may be transferred to a water molecule to

form  $\text{H}_3\text{O}^+$ . However, the proton can only migrate by hopping from site to site across the Pyr-rGO film surface. Therefore, the impedance was relatively high at low RH range since the weak ion transport was on account of the noncontinuous and low water coverage. At middle RH (34–74% RH), the appearance of a semicircle in the Nyquist plots suggested the existence of  $\text{H}^+$  hopping conduction. According to the ion transfer mechanism of Grothuss,<sup>[39]</sup> the initial and final state are the same and the energies are also balanced, thus the ion transfer was quite easy. Moreover, at this RH level, more water molecules can be adsorbed onto Pyr-rGO film due to the hydrophilic sulfonic groups of pyranine. The adsorbed water molecules can form one or several serial water layers which accelerated the transfer of  $\text{H}^+$  or  $\text{H}_3\text{O}^+$ , resulting in a swift decrease in the impedance at this stage. At high RH range (75–95% RH), the Nyquist plots exhibited a semicircle shape with a short straight line in the low-frequency region. As the RH increased, the straight line grew longer while part of the semicircle disappeared. The short straight line represented Warburg impedance, caused by the diffusion of the ions in the sensing material / electrode interface. At high RH range, apart from chemical adsorption, physical adsorption has become the main adsorption method. Thus, more serial water layers were formed to further accelerate the ions transfer, and the water molecules can permeate into the Pyr-rGO film to induce electrolytic conduction. Therefore, the impedance continuously decreased at high RH range.<sup>[23]</sup>

### 5.2.2. Electron-Transport Mechanism

The adsorption of water into the structure of the sensing element triggers changes in the electronic structure of the system. This mechanism was exploited in devices based on both optical and electrical readout. For instance solvatochromism effect occurs when the energy of intramolecular electronic transitions in organic molecules is sensitive to changes in the polarity of the surrounding medium. This effect produces reversible color changes of solvated organic molecules as a function of the solvent polarity. Electrical readouts (e.g., resistance, conductivity or impedance) can be exploited when water molecules act as dopants of the sensing material, or in other words, when there are charge-transfer processes.

In 2018, Ascher et al.<sup>[27b]</sup> reported the first COFs that change their electronic structure reversibly depending on the surrounding atmosphere (Figure 5b). The strong donor–acceptor contrast in the composing moieties, i.e., tetraphenylpyrene and thieno[3,2-b]thiophene, yielded nanoporous Py-TT COFs with a pronounced solvatochromism effect. These COFs can act as solid-state supramolecular solvatochromic sensors that displayed a strong color change when exposed to humidity or solvent vapors, because of its sensitivity to vapor at different concentrations and solvent polarity. The excellent accessibility of the pores in vertically oriented films resulted in ultrafast response times below 200 ms for a 360 nm-thick COF, outperforming commercially available humidity sensors by more than an order of magnitude. As the solvent molecules needed to diffuse through the entire film in order to saturate the solvatochromic color change, the authors anticipated a strong correlation between film thickness and response time. Indeed, both

response times were shorter for thinner films, whereby the fastest response of 110 ms/ 90 ms (rise/fall) was achieved upon using a 160 nm-thick COF film. Additionally, the Py-TT COF films displayed excellent reversibility, reproducibility during repeated switching (i.e., over at least 4000 humidity and solvent vapor switching cycles) and long lifecycle (i.e., storage in ambient air for 250 days). Furthermore, the authors excluded any chemical or structural changes during the humidity sensing process that might alter the coupling between the building blocks or COF layers. As a final proof of concept, the authors employed the COF thin film as a vapor-sensitive light filter, where a continuous read-out was realized in combination with a green light-emitting diode (LED) and a light-dependent resistor.<sup>[27b]</sup>

Tang et al. reported the fabrication of a supramolecular free-standing film of GO and aniline (GOA) and studied its humidity dependence via direct current (DC) conductance.<sup>[22]</sup> Putty-like supramolecular GOA was generated after stirring a mixture of GO and aniline for several hours. The excellent processability made GOA to be easily customized into the desired shape. Importantly, GOA humidity sensors can be mass-produced by cutting large-area GOA film, which is convenient and low cost for sensor production. The authors prepared freestanding GOA films with a size of  $1.5 \times 1 \times 0.14 \text{ mm}^3$  which were then coated with silver colloid on both edges and connected with silver wire for sensing analysis. Freestanding GOA films showed an excellent performance in terms of broad operating range (from 10% to 90% RH), fast response and recovery times (i.e.,  $\approx 50 \text{ ms}$ ), high selectivity in the presence of other gases and long lifecycle (i.e., at least 4 weeks). The internal hydrophobicity and surface moderate hydrophobicity of GOA not only ensured the effective connection of the conductive channels but also reduced the time of adsorption and desorption, which was one of the keys to achieving ultrafast response. Besides, the authors ascertained by means of microscopy the absence of thickness changes during the sensing process, suggesting that the water molecules cannot enter the interior of the GOA material and the changes in conductance are purely a result of the electronic process. Within the GOA structure, there was a combination between  $\pi$ – $\pi$  interaction and hydrogen bond between GO sheet and aniline. Both, GO and aniline, which have large numbers of hydrophilic oxygen groups and hydrophilic amino groups, respectively, can easily form hydrogen bonds with water molecules. At low humidity, the adsorbed water molecules formed a bridge between isolated oxygen functional groups and amino groups on the surface of the GOA film. As a result, the isolated conductive regions, where  $\text{sp}^2$ -hybridized carbon was partially reserved in the oxidation process, will form interconnected conductive channels. As the humidity increased to a certain extent, the aggregated water clusters formed a water film on the GOA surface. The conductive behavior of water film became dominant at high humidity. Additionally, the authors also assessed the sensing performance of GOA by impedance spectroscopy. The Nyquist plot displayed a semicircle due to the intrinsic impedance of the film at low humidity. With the increasing RH, the complex impedance spectra showed a smaller semicircle, associated with a decrease in resistance and reactance, that is, the enhancement in conductance and capacitance, in full agreement with the interaction (charge-transfer process) of water molecules with the sensing film.<sup>[22]</sup>

In order to tackle the current disadvantages of optical humidity sensors, including high cost, weak luminescence, slow response time and low sensitivity, Gao et al., reported the fabrication of a perovskite/zeolite composite as a fluorescent humidity sensor.<sup>[41]</sup> This hybrid material is based on the combination of a perovskite, Cs<sub>4</sub>PbBr<sub>6</sub>, which acts as ad hoc receptor of moisture and a zeolite, FAU-Y, which acts both as a support of Cs<sub>4</sub>PbBr<sub>6</sub> nanoparticles as well as a hygroscopic substrate material. The porous network and relatively large water adsorption capacity of FAU-Y allowed to increase the contact between water and the water-sensitive Cs<sub>4</sub>PbBr<sub>6</sub>, achieving the highest fluorescence response value and sensitivity to date among metal halide perovskites.<sup>[41]</sup>

Although they have not been exploited yet as supramolecular humidity sensors, in an analogous manner to the perovskite/zeolite composite reported by Gao et al.,<sup>[41]</sup> semiconductors could be used as a hygroscopic substrate materials due to the charge-trapping effect.<sup>[42]</sup> It has been reported that water can be trapped underneath graphene and an adjacent dielectric, influencing the operation of the device.<sup>[42a]</sup> Similarly, water molecules can diffuse into nanovoids in semiconducting polymeric films of indacenodithiophene-co-benzothiadiazole, acting as charge traps and interfering with charge transport, thereby promoting charge mobility degradation.<sup>[42b]</sup> Albeit the trapping effect can be detrimental for some applications and should not be neglected, it can be seen as a synergistic effect for the fabrication of highly efficient humidity sensors

### 5.2.3. Electron/Proton Mixed Transport Mechanism

Yan et al.<sup>[15b]</sup> reported the fabrication of an exhaled humidity sensor based on a new synthetic redox conducting supramolecular ionic material (SIM) for the real-time monitoring of the respiratory rate. The conducting SIM was prepared by ionic self-assembly in aqueous solutions of electroactive 2,2'-azino-bis(3-ethylbenzothiazoline-6-sulfonic acid) (ABTS) and 1,10-bis(3-methylimidazolium-1-yl) decane (C<sub>10</sub>(mim)<sub>2</sub>). As a result of the high hygroscopicity and water stability arising from the ionic and hydrophobic interactions between two building blocks (i.e., ABTS and C<sub>10</sub>(mim)<sub>2</sub>), the SIM-based chemiresistive humidity sensor exhibited at a relatively low polarized potential (i.e., 0.5 V), high sensitivity (less than 0.1% RH), broad operation range (i.e., 11% to 86% RH), fast response time (i.e., ≈37 ms), long lifecycle (i.e., 10 months) and high selectivity in the presence of the main components of respiratory gas, such as nitrogen, oxygen, carbon dioxide validating the SIM-based humidity sensors' appropriateness for RR monitoring.<sup>[15b]</sup> The sensing mechanism was explained as follows: under N<sub>2</sub> atmosphere, the SIM exhibited a very low conductivity (i.e., 1.03 × 10<sup>-13</sup> S cm<sup>-1</sup>), comparable to that of an insulator. This result was consistent with the fact that the SIM lacked localized π electrons, and due to the relatively large size of C<sub>10</sub>(mim)<sub>2</sub>, it was difficult to accommodate as a counterion for the electron self-exchange of ABTS in the solid state. When the SIM was exposed to moisture, its electronic conductivity sharply increased. This increase resulted from the ionization of the adsorbed water molecules and further assistance of the electron self-exchange of ABTS. Importantly, the authors reported

the synthesis of another ionic material (i.e., C<sub>10</sub>(mim)<sub>2</sub>(PF<sub>6</sub>)<sub>2</sub>) without an electroactive building block. This material showed a relatively weak dependence of the electronic conductivity on the humidity level and essentially supported the proposed redox-based mechanism.<sup>[15b]</sup>

More recently, Turetta et al.<sup>[13]</sup> reported the fabrication of a novel [1]benzothieno[3,2-b][1]benzothiophene derivative, designed with a conjugated benzothienobenzothiophene (BTBT) core and hygroscopic oligoethylene glycol (OEG) side chains (i.e., OEG-BTBT) (Figure 5c). The BTBT cores self-assembled to form crystalline films displaying a highly delocalized electronic structure capable of efficient electronic transport at long distances. These films were assessed as chemiresistive humidity sensors, exhibiting high sensitivity (i.e., high current ratios, >10<sup>4</sup>), broad operation range (10–80% RH), low operating voltage (i.e., 2 V), complete reversibility upon RH increase and decrease, fast response and recovery time (i.e., ≈100–500 ms), and good reproducibility. By means of impedance spectroscopy, the authors observed that at low humidity (RH ≈10%), OEG-BTBT exhibited a response toward humidity predominantly capacitive with a high-resistance contribution. However, as RH increases to ≈97%, the mixed electronic/protonic (H<sup>+</sup>) conduction governed the electrical response of such films. Such ionic conduction was attributed to the dissociated H<sup>+</sup> from atmospheric water molecules at the ethylene glycol moieties of OEG-BTBT that are transported upon the effect of the voltage bias, resulting in an ionic conductivity of σ<sub>i</sub> ≈ 2 × 10<sup>-3</sup> S cm<sup>-1</sup>, which is similar to the values reported for other organic H<sup>+</sup> conductors. Grazing-incidence wide-angle X-ray scattering (GIWAXS) measurements made it possible to ascertain the absence of structural changes in the OEG-BTBT crystalline structure to the changes in humidity level enabling to conclude that the sensing process was solely governed by electronic/ionic-transport mechanism. Importantly, the authors shed some light on other factors that could influence the performance of chemiresistive humidity sensors and such, should be properly determined and optimized. Among those, they observed that the adsorption of atmospheric water can be synergistically favored by employing thin films deposited on hydrophilic SiO<sub>2</sub> substrates. The chemiresistor response was also shown to depend on the device geometry and electrode configuration (bottom-contact versus top-contact SiO<sub>2</sub> test patterns, position with respect to the film surface, channel length, and thin-film thickness). Finally, comparative studies performed on hole-conducting BTBT cores decorated with alkyl side chains (C8-BTBT) exhibited no significant humidity response, which endorsed the key role played by the hygroscopic OEG moieties.<sup>[13]</sup>

To improve the sensing performances of rGO, Anichini et al.<sup>[27a]</sup> reported a novel chemiresistive humidity sensor based on a simple chemical modification of rGO with hydrophilic moieties, i.e., triethylene glycol chains. 2-[2-(2-Methoxyethoxy)-ethoxy]ethylamine (NTEG) was chosen as it can interact with water molecules forming weak, thus reversible, hydrogen bonding when compared to carbonyls, carboxylic acids, and hydroxyls. As control material, rGO was functionalized with decylamine (rGO-decylamine), which did not possess triethylene glycol chains. Such a hybrid material (i.e., rGO-NTEG), due its higher hydrophilicity, exhibited an outstandingly improved sensing performance compared to pristine rGO or

and rGO-decylamine in terms of high sensitivity (31% increase in electrical resistance when humidity is shifted from 2% to 97%), an ultrafast response (25 ms) and recovery in the sub-second timescale, low hysteresis (1.1%), excellent repeatability and lifecycle, as well as high selectivity toward moisture in the presence of other gases such as methanol, ethanol, acetone or chloroform. The use of humidity-dependent PXRD proved that the functional groups present on the rGO surface had a low impact on the structural changes of the materials when they were exposed to a humid environment. Importantly, the authors unravel the physical origin of the sensing mechanism by means of force field MD simulations. The presence of chemically attached molecules can favor or disfavor the interaction of water molecules with the graphene surface, leading to different electronic behavior.<sup>[27a]</sup>

Supramolecular humidity sensors governed by charge-transport changes are mainly exploited via electrical readouts. In general, most of these systems exhibit a broader operation range than the supramolecular nanostructures governed by morphological and structural changes. For instance, 2-[2-(2-methoxyethoxy)-ethoxy]ethylamine can operate between 2% and 97% RH and exhibit the highest responsiveness (25 and 127 ms as response and recovery time).

### 5.3. Hybrid Mechanism

Finally, the last mechanism can be classified as a hybrid mechanism when humidity triggers both structural and charge-transport changes in the supramolecular nanostructures. These changes were monitored by both optical and electrical readout.

Hwang, et al.<sup>[32]</sup> reported the fabrication of composite films based on poly(dopamine)-treated graphene oxide/poly(vinyl alcohol) (dGO/PVA). By design the PVA chains should strongly bind on the surface of GO by hydrogen bonding. During the polymerization of dopamine on the GO surface, poly(dopamine) acted as a reducing agent of GO. Poly(dopamine) formed a strong adhesion layer with GO via hydrogen bonding between amine and hydroxyl groups of poly(dopamine) and hydroxyl groups of GO as well as  $\pi$ - $\pi$  of GO interaction between catechol and small graphitic domains of GO. The dGO served as a moisture barrier for water-soluble PVA, and dGO/PVA composites showed a lower maximum swelling ratio (around 120% at 3 or 5 wt% dGO) compared to a neat PVA film. Importantly the dGO/PVA composite films have shown to be efficient humidity sensors over the operation range of 40–100% RH, much broader than pristine PVA (between 98% and 99% RH). If the swelling mechanism was the only mechanism of humidity sensing in dGO/PVA composites, the film resistance would increase proportionally to the RH. The swelling of the polymer matrix due to moisture adsorption would lead to an increase in electrical resistance as the electrically conductive network formed by dGO nanosheets becomes disrupted. However, the authors observed the opposite trend. When the surface of a dGO/PVA film was exposed to water molecules, adsorption occurred, and capillary condensation of water produced a proton ( $H^+$ ). This proton can be a carrier for the improvement of electrical conduction in dGO/PVA films, and more protons are produced when the sensing material was exposed to more

humidity in the testing system.<sup>[32]</sup> Remarkably, the samples were more moisture-sensitive at lower RH values. This may be due to the fact that proton saturation for conduction was more readily reached in low humidity regions where there was no considerable swelling level of the polymer.<sup>[32]</sup>

By means of a layer-by-layer assembly, Zhang et al.<sup>[30a]</sup> reported the fabrication of a nanocomposite film based on the alternate deposition of rGO and the polymer poly(diallylimethylammonium chloride) (PDDA) on a flexible polyimide substrate with interdigitated microelectrodes. This composite was exploited as a chemiresistive humidity sensor, exhibiting a broad operation range (11–97% RH) at room temperature, fast response–recovery times, good repeatability and long lifecycle (i.e., at least 60 days). The electron transport through the PDDA/rGO nanocomposite exhibited p-type semiconducting behavior and was dominated by positive charge carriers (holes). Water molecules, though, served as electron donors. At low RH, the chemisorbed water molecules caused a reduction of hole concentration in the p-type RGO sheets, increasing film resistance. At high RH, the multilayer adsorbed water molecules may be ionized to produce hydronium ions ( $H_3O^+$ ) as charge carriers. According to the Grotthuss model introduced before,<sup>[39]</sup> the protons are transported via ionic conductivity causing a decrease in sensor resistance. However, the authors did not observe such behavior because water molecules entered into the multilayer film leading to a swelling effect. The swelling of the PDDA/rGO increased the interlayer rGO distance, increasing the sensor resistance. Consequently, there was a trade-off between humidity-induced swelling effect and ionic conduction occurring in the humidity sensor. In the present case, the governing sensing mechanism was attributed to the p-type semiconducting properties of RGO at low RH, and the interlayer swelling of PDDA/rGO film at high RH rather than the ionic conductivity.<sup>[30a]</sup>

Samai et al.<sup>[30b]</sup> reported the spontaneous self-assembly of a two-component gelator based on the anionic azobenzene dicarboxylate (AZNa) and the cationic cetyltrimethylammonium bromide (CTAB). The mechanism of self-assembly was mainly driven by the electrostatic interactions of anionic AZNa with cationic CTAB in addition to the  $\pi$ - $\pi$  stacking of the AZNa aromatic rings. This supramolecular assembly formed a stimuli-responsive hydrogel which was successfully employed in the fabrication, for the first time, of highly sensitive humidity sensors. A film of the aforementioned gel was immobilized on gold interdigitated electrodes and its response to humidity changes was followed by impedance spectroscopy. A decreasing trend in the impedance, or in other words, an increase in conductivity, with the increase of the RH was observed. Although some swelling of the hydrogel can occur due to the water uptake, the increase in conductivity is most probably related to the electronic changes that water triggers within the supramolecular assembly. Besides, the authors studied the impedimetric dependence of three different gel concentrations. Increasing the gel concentration yielded to lower impedance values due to their higher relative permittivity.<sup>[30b]</sup>

Schoelch et al.<sup>[28]</sup> reported the fabrication of a colorimetric humidity memory sensor based on the simple physical mixing of a red-colored azo dye (i.e., 2-(ethyl(4-((4-nitrophenyl)diazenyl)phenyl)amino)ethan-1-ol (DR1) or *N,N*-diethyl-4-((4-nitrophenyl)diazenyl)aniline (DEA)) and a host polymer matrix (i.e., poly(vinylpyrrolidone) (PVP)). These materials were easily

painted onto a wide variety of surfaces and underwent a remarkable color change upon exposure to various thresholds of levels of RH. Interestingly, the strong color change, easily visible as a red-to-orange color switch, was locked in until inspection, making these materials humidity memory materials. With a simple moderate heating treatment, the initial state of the materials was recovered. As sensing mechanism, the authors claimed that when the thin films were exposed to humid air, water penetrated readily into the thin film and interacted with the PVP chains based on their H-bond donating properties. Utilizing neutron reflectometry, it was found that water can easily penetrate into thin polymer films. Besides, gravimetric studies revealed that one *n*-vinyl-2-pyrrolidone unit can accommodate up to 9.5 water molecules in the swollen state. When PVP polymer was swollen by water molecules, the phase separation of DR1 and DEA dyes was triggered, as both are insoluble in water. This led to the antiparallel stacking of molecular dipoles, often referred to as H-aggregation. Finally, using Raman spectroscopy the authors supported the hypothesis that the orange (“wet”) state being observed was an aggregated state of DR1 or DEA molecules. Therefore, the exposure to humidity in this system led on the one hand to the swelling of the PVP polymer and on the other hand to the shrinking of DR1 or DEA molecules<sup>[28]</sup>

Chakraborty et al.<sup>[29b]</sup> reported the design and fabrication of a Pt(II)-based MSP with carboxylic acid groups (polyPtC) and investigated the humidity-responsive properties of the polymer. The authors selected this design because the  $d_{\pi}-d_{\pi}$  metal–metal interaction and/or  $\pi-\pi$  stacking between the terpyridine-containing  $\pi$ -systems lead to the triplet state luminescence properties. The increase in RH triggered the inclusion of water molecules inside the polymer chains through the interaction with the hydrophilic metal cation center or the carboxylic acid groups. The authors demonstrated by PXRD characterization that the incorporated water molecules into the polyPtC structure decreased the Pt–Pt interaction and subsequently increased the interchain Pt–Pt distance from 4.05 to 4.41 Å. Accordingly, the emission spectrum of polyPtC diminished with the increase of RH. Moreover, to demonstrate that the water molecules can form a water channel along with the polymer chain, enhancing the ionic conductivity of the polymer film, a polyPtC film was prepared on a chemiresistor. The authors proved that when the humidity gradually increased from 25% to 100% RH, the enhancement of the conductance ( $1/R$ ) was observed simultaneously.<sup>[29b]</sup>

## 6. Conclusions and Outlook

We have presented the key concepts for achieving state-of-the-art humidity sensing by using supramolecular nanostructures. Various supramolecular materials have been discussed here to provide a critical review of their performance along with a discussion on possible application areas. The sensing mechanisms in different systems have been discussed in a case-by-case manner along with their operating principles and corresponding key performance indicators (KPIs). Supramolecular humidity sensors, although still in their infancy, have already shown great potential outperforming many of the current commercial devices in terms of sensitivity, responsiveness

and selectivity. The poor selectivity of pristine materials such as ceramic materials, carbon-based materials, and organic/polymeric materials hinders their practical application as humidity sensors, especially in complex ambient atmospheres. By taking full advantage of the noncovalent nature of moisture–materials interactions, which guarantee fast response and signal recovery, and their high selectivities that can be achieved via the ad hoc molecular design of supramolecular receptors, the next-generation of sensory materials and technologies can be produced.

Among the different operating principles, electrical readout (including resistive, impedimetric, and piezoresistive sensors) is revealed to be the most popular one, not only for laboratory research but also for practical applications. Electrical sensing devices present several advantages such as fabrication methods compatible with industrial practices, low-cost and large-scale production, adaptability to different types of circuits, and ease of fabrication and measurement setup. While the market is currently dominated by humidity sensors that rely primarily on electrical sensing principles, developments in optical sensors also show great potential owing to their unique benefits including simplicity and the lack of need for a power supply as well as their portability and simple yet powerful data collection with smart phones and digital cameras.

Regarding the sensing mechanism, for the first time, we have categorized the different sensing materials according to the changes triggered by their interaction with moisture. A deeper understanding of the sensing mechanism is needed to boost the performance of supramolecular-based humidity sensors through the optimization of the chemical structures of the supramolecular receptors and therefore the control of water–material interactions.

The optimization of other factors has shown to be key to achieving state-of-the-art performance, including device engineering through a careful choice of its geometry, electrode configuration, material thickness and substrate hydrophilicity/hydrophobicity. Nowadays, thin-film-based humidity sensors, for both electrical and optical readout, are extensively utilized because of their cost-effectiveness, design flexibility and quick deposition rate. Based on recent development trends we envision that a strong focus will be placed not only on the fabrication of novel materials but also on the advance of the current sensors in terms of flexibility, degradability and durability. With further developments in substrate materials, functional inks, and process technologies, flexible humidity sensors with superior sensitivity and operation range will be possible. Flexible humidity sensors will find numerous applications in which the sensing elements either need to be bent or stretched, as in wearable applications. The development of wearable sensors will be pivotal for the real-time health monitoring ultimately allowing the early diagnosis of diseases. Fortunately, typical process technologies used in the fabrication of flexible humidity sensors harness the advantages of spray-coating and roll-to-roll manufacturing, thereby reducing time and production costs.

Although at the laboratory scale there are many reports in the literature on high-performing supramolecular-based humidity sensors, the commercialization of these products is still far from reality. Demonstrations of practical applications of the proposed humidity sensors are still rather limited. We strongly believe that the performance of the existing sensors



and the upcoming sensors need to be well explored for robust applications. Temperature calibration and selectivity assessment are mandatory to guarantee reliable measurements. On the other hand, the multifunctional and multiresponsive nature of supramolecular nanostructures can offer some key advantages compared to more conventional materials, for the development of devices exhibiting a greater functional complexity and multifunctionality, even for example in the framework of sensing of multiple analytes (i.e., multiplexing). Theoretical studies and computational simulations may aid in designing more reliable humidity sensors beyond the state of the art.

Besides, fields of application of humidity sensors are fast expanding. For instance, detection of water in protic solvents is still especially challenging. Developing new strategies to detect water in the near-infrared (NIR) region could open doors to new biological advancements. Human-body-related humidity detection, including respiratory behavior, speech recognition, skin moisture, noncontact switch, and diaper monitoring, needs some new features as compared with environmental humidity sensors, such as flexibility, fast response and recovery speed, and nontoxicity. Differently, moisture memory devices, which only recover their initial state after an external stimulus, have proven to be extremely useful as self-indicative smart materials that can be incorporated in chemical bottles, food packaging, etc.

Humidity sensing has proven to be key to aiding several sectors of our society, offering solutions to issues in medical (early) diagnostics and monitoring, industrial safety, household comfort, lifetime and lifecycle of materials as well as environmental and food surveillance, ultimately improving the quality of our lives on this planet.

## Acknowledgements

The authors acknowledge funding from the European Commission through the ERC project SUPRA2DMAT (GA-833707) and the Agence Nationale de la Recherche through the Interdisciplinary Thematic Institute SysChem via the IdEx Unistra (ANR-10-IDEX-0002) within the program Investissement d'Avenir, the International Center for Frontier Research in Chemistry (icFRC) and the Institut Universitaire de France (IUF).

## Conflict of Interest

The authors declare no conflict of interest.

## Keywords

humidity sensors, sensing mechanism, supramolecular nanostructures, water receptors

Received: September 23, 2022

Revised: November 1, 2022

Published online:

[1] H. Farahani, R. Wagiran, M. N. Hamidon, *Sensors* **2014**, *14*, 7881.

[2] M. Srbinovska, C. Gavrovski, V. Dimcev, A. Krkoleva, V. Borozan, *J. Clean Prod.* **2015**, *88*, 297.

- [3] Y.-T. Jao, P.-K. Yang, C.-M. Chiu, Y.-J. Lin, S.-W. Chen, D. Choi, Z.-H. Lin, *Nano Energy* **2018**, *50*, 513.
- [4] S. Gupta Chatterjee, S. Chatterjee, A. K. Ray, A. K. Chakraborty, *Sens. Actuators, B* **2015**, *221*, 1170.
- [5] L. Yu, Q. Zheng, H. Wang, C. Liu, X. Huang, Y. Xiao, *Anal. Chem.* **2020**, *92*, 1402.
- [6] F. Bibi, C. Guillaume, N. Gontard, B. Sorli, *Trends Food Sci. Technol.* **2017**, *62*, 91.
- [7] H. Yan, Z. Liu, R. Qi, *Nano Energy* **2022**, *101*, 107591.
- [8] Y. Lu, G. Yang, Y. Shen, H. Yang, K. Xu, *Nano-Micro Lett.* **2022**, *14*, 150.
- [9] T. A. Blank, L. P. Eksperianova, K. N. Belikov, *Sens. Actuators, B* **2016**, *228*, 416.
- [10] a) J.-M. Tulliani, B. Inserra, D. Ziegler, *Micromachines* **2019**, *10*, 232; b) M. Jian, C. Wang, Q. Wang, H. Wang, K. Xia, Z. Yin, M. Zhang, X. Liang, Y. Zhang, *Sci. China Mater.* **2017**, *60*, 1026.
- [11] B. Adhikari, S. Majumdar, *Prog. Polym. Sci.* **2004**, *29*, 699.
- [12] R. Furlan de Oliveira, V. Montes-García, A. Ciesielski, P. Samori, *Mater. Horiz.* **2021**, *8*, 2685.
- [13] N. Turetta, M.-A. Stoeckel, R. Furlan de Oliveira, F. Devaux, A. Greco, C. Cendra, S. Gullace, M. Gicevičius, B. Chattopadhyay, J. Liu, G. Schweicher, H. Siringhaus, A. Salles, M. Bonn, E. H. G. Backus, Y. H. Geerts, P. Samori, *J. Am. Chem. Soc.* **2022**, *144*, 2546.
- [14] W. Jeong, J. Song, J. Bae, K. R. Nandanapalli, S. Lee, *ACS Appl. Mater. Interfaces* **2019**, *11*, 44758.
- [15] a) X. Li, Z. Zhuang, D. Qi, C. Zhao, *Sens. Actuators, B* **2021**, *330*, 129239; b) H. Yan, L. Zhang, P. Yu, L. Mao, *Anal. Chem.* **2017**, *89*, 996; c) Y. Ma, X. Hu, S. Li, Y. He, Z. Xia, K. Cai, *Macromol. Mater. Eng.* **2022**, *307*, 2100686; d) S. A. Iyengar, P. Srikrishnarka, S. K. Jana, M. R. Islam, T. Ahuja, J. S. Mohanty, T. Pradeep, *ACS Appl. Electron. Mater.* **2019**, *1*, 951.
- [16] Z. M. Rittersma, *Sens. Actuator, A* **2002**, *96*, 196.
- [17] J. Xue, Y. Ge, Z. Liu, Z. Liu, J. Jiang, G. Li, *ACS Appl. Mater. Interfaces* **2022**, *14*, 10836.
- [18] M. A. Squillaci, X. Zhong, L. Peyruchat, C. Genet, T. W. Ebbesen, P. Samori, *Nanoscale* **2019**, *11*, 19315.
- [19] M. Li, Q. Lyu, L. Sun, B. Peng, L. Zhang, J. Zhu, *ACS Appl. Mater. Interfaces* **2020**, *12*, 39665.
- [20] U. Mogera, M. Gedda, S. J. George, G. U. Kulkarni, *ACS Appl. Mater. Interfaces* **2017**, *9*, 32065.
- [21] M. del Pozo, C. Delaney, C. W. M. Bastiaansen, D. Diamond, A. P. H. J. Schenning, L. Florea, *ACS Nano* **2020**, *14*, 9832.
- [22] M. Tang, C. Zhang, J.-Y. Zhang, Q.-L. Zhao, Z.-L. Hou, K.-T. Zhan, *Phys. Status Solidi A* **2020**, *217*, 1900869.
- [23] Z. Chen, Y. Wang, Y. Shang, A. Umar, P. Xie, Q. Qi, G. Zhou, *Sci. Rep.* **2017**, *7*, 2713.
- [24] a) M. A. Squillaci, M.-A. Stoeckel, P. Samori, *Nanoscale* **2019**, *11*, 19319; b) T. Li, L.-X. Zhang, Y. Xing, H. Xu, Y.-Q. Yue, Q. Li, H. Dong, H.-Y. Wang, Y.-Y. Yin, *Inorg. Chem. Commun.* **2019**, *108*, 107541.
- [25] N. Herzer, H. Guneyusu, D. J. D. Davies, D. Yildirim, A. R. Vaccaro, D. J. Broer, C. W. M. Bastiaansen, A. P. H. J. Schenning, *J. Am. Chem. Soc.* **2012**, *134*, 7608.
- [26] M. A. Squillaci, A. Cipriani, M. Melucci, M. Zambianchi, G. Caminati, P. Samori, *Adv. Electron. Mater.* **2018**, *4*, 1700382.
- [27] a) C. Anichini, A. Aliprandi, S. M. Gali, F. Liscio, V. Morandi, A. Minoia, D. Beljonne, A. Ciesielski, P. Samori, *ACS Appl. Mater. Interfaces* **2020**, *12*, 44017; b) L. Ascherl, E. W. Evans, M. Hennemann, D. Di Nuzzo, A. G. Hufnagel, M. Beetz, R. H. Friend, T. Clark, T. Bein, F. Auras, *Nat. Commun.* **2018**, *9*, 3802.
- [28] S. Schoelch, J. Vapaavuori, F.-G. Rollet, C. J. Barrett, *Macromol. Rapid Commun.* **2017**, *38*, 1600582.
- [29] a) Y.-Y. Yin, L.-X. Zhang, X. Wang, B.-L. Zhang, X.-Q. Gong, L. Liu, R.-H. Sun, *Inorg. Chem. Commun.* **2019**, *100*, 38; b) C. Chakraborty,

- U. Rana, S. Moriyama, M. Higuchi, *ACS Appl. Polym. Mater.* **2020**, 2, 4149.
- [30] a) D. Zhang, J. Tong, B. Xia, *Sens. Actuators, B* **2014**, 197, 66; b) S. Samai, C. Sapsanis, S. P. Patil, A. Ezzeddine, B. A. Moosa, H. Omran, A.-H. Emwas, K. N. Salama, N. M. Khashab, *Soft Matter* **2016**, 12, 2842.
- [31] S.-Y. Son, M.-S. Gong, *Sens. Actuators, B* **2002**, 86, 168.
- [32] S.-H. Hwang, D. Kang, R. S. Ruoff, H. S. Shin, Y.-B. Park, *ACS Nano* **2014**, 8, 6739.
- [33] U. Mogera, A. A. Sagade, S. J. George, G. U. Kulkarni, *Sci. Rep.* **2014**, 4, 4103.
- [34] M. A. Squillaci, L. Ferlauto, Y. Zagranyski, S. Milita, K. Müllen, P. Samorì, *Adv. Mater.* **2015**, 27, 3170.
- [35] X. Yu, X. Ge, L. Geng, H. Lan, J. Ren, Y. Li, T. Yi, *Langmuir* **2017**, 33, 1090.
- [36] X.-M. Jiang, Z.-B. Yan, D. Liu, K.-F. Wang, G.-C. Guo, S.-Z. Li, J.-M. Liu, *Chem. Asian J.* **2014**, 9, 2872.
- [37] P. G. M. Mileo, T. Kundu, R. Semino, V. Benoit, N. Steunou, P. L. Llewellyn, C. Serre, G. Maurin, S. Devautour-Vinot, *Chem. Mater.* **2017**, 29, 7263.
- [38] S.-Y. Peng, L.-S. Yang, M.-S. Yao, L.-S. Yu, *New J. Chem.* **2018**, 42, 1787.
- [39] B. M. Kulwicki, *J. Am. Ceram. Soc.* **1991**, 74, 697.
- [40] S. Borini, R. White, D. Wei, M. Astley, S. Haque, E. Spigone, N. Harris, J. Kivioja, T. Ryhänen, *ACS Nano* **2013**, 7, 11166.
- [41] Y.-J. Gao, G. Romolini, H. Huang, H. Jin, R. A. Saha, B. Ghosh, M. De Ras, C. Wang, J. A. Steele, E. Debroye, J. Hofkens, M. B. J. Roeffaers, *J. Mater. Chem. C* **2022**, 10, 12191.
- [42] a) E. J. Olson, R. Ma, T. Sun, M. A. Ebrish, N. Haratipour, K. Min, N. R. Aluru, S. J. Koester, *ACS Appl. Mater. Interfaces* **2015**, 7, 25804; b) A. M. Zeidell, D. S. Filston, M. Waldrip, H. F. Iqbal, H. Chen, I. McCulloch, O. D. Jurchescu, *Adv. Mater. Technol.* **2020**, 5, 2000390.



**Verónica Montes-García** obtained her Ph.D. degree from the University of Vigo. Currently, she is working as a postdoctoral researcher in the group of Prof. Paolo Samorì in the Institut de Science et d'Ingénierie Supramoléculaires (I.S.I.S.). Her research is focused on the synthesis and characterization of new hybrid materials for the creation of new multifunctional systems with applications in the fields of detection, catalysis and energy.



**Paolo Samorì** is Distinguished Professor at the University of Strasbourg and Director of the Institut de Science et d'Ingénierie Supramoléculaires. He is Fellow of the Royal Society of Chemistry (FRSC), Fellow of the European Academy of Sciences (EURASC), Member of the Academia Europaea, Foreign Member of the Royal Flemish Academy of Belgium for Science and the Arts (KVAB) and Senior Member of the Institut Universitaire de France (IUF). His research interests comprise nanochemistry, supramolecular sciences, materials chemistry with specific focus on graphene and other 2D materials, functional organic/polymeric and hybrid nanomaterials for application in optoelectronics, energy, and sensing.